TALLINN UNIVERSITY OF TECHNOLOGY
SCHOOL OF ENGINEERING

Department of Civil Engineering and Architecture

CRYSTALLIZATION KINETICS OF CALCIUM SULPHATE IN THE PRESENCE OF METAL IONS

KALTSIUMSULFAADI KRISTALLUMISE KINEETIKA METALLIIOONIDE JUURESOLEKUL

MASTER THESIS

Student	John Moses Budatala
Student code	184546EABM
Supervisor at TUT, Tallinn	Prof. Karin Pachel
Supervisor at UCT, Prague	Ing. Marek Šír

Tallinn, 2020

AUTHOR'S DECLARATION

Hereby I declare, that I have written this thesis independently.
No academic degree has been applied for based on this material.
All works, major viewpoints and data of the other authors used in this thesis have been referenced.

" 27" May 2020

Author: .....
/signature /

Thesis is in accordance with terms and requirements

"27 " May 2020

Supervisor: ….....
/signature/

Supervisor: ….....
/signature/

Accepted for defence

"27 " May 2020

Chairman of theses defence commission: Karin Pachel
/name and signature/

Non-exclusive Licence for Publication and Reproduction of GraduationTthesis[1]

I, John Moses Budatala (date of birth: 24/04/1995) hereby

1. grant Tallinn University of Technology (TalTech) a non-exclusive license for my thesis- 'CRYSTALLIZATION KINETICS OF CALCIUM SULPHATE IN THE PRESENCE OF METAL IONS', supervised by

Marek Šír

Karin Pachel

1.1 reproduced for the purposes of preservation and electronic publication, incl. to be entered in the digital collection of TalTech library until expiry of the term of copyright;

1.2 published via the web of TalTech, incl. to be entered in the digital collection of TalTech library until expiry of the term of copyright.

1.3 I am aware that the author also retains the rights specified in clause 1 of this license.

2. I confirm that granting the non-exclusive license does not infringe third persons' intellectual property rights, the rights arising from the Personal Data Protection Act or rights arising from other legislation.

---

[1] Non-exclusive Licence for Publication and Reproduction of Graduation Thesis is not valid during the validity period of restriction on access, except the university`s right to reproduce the thesis only for preservation purposes.

_____ (signature)

_____ (date)

Department of Civil Engineering and Architecture

THESIS TASK

Student: John Moses Budatala; 184546EABM

Study programme: Environmental Engineering and Management (EABM03)

Supervisor(s): Ing. Marek Šír, Academic staff at UCT Prague;

Prof. Karin Pachel, Program Director, Environmental Engineering and Management

Thesis topic:

In English : CRYSTALLIZATION KINETICS OF CALCIUM SULPHATE IN THE PRESENCE OF METAL IONS

In Estonian : KALTSIUMSULFAADI KRISTALLUMISE KINEETIKA METALLIIOONIDE JUURESOLEKUL

Thesis main objectives:

- Design and perform a series of jar tests to determine crystallization kinetics of calcium sulphate dihydrate at laboratory temperature
- Test crystallization phenomena of calcium sulphate dihydrate in the presence of selected metals. Based on the measured data, evaluate how the morphology of calcium sulfate crystals formed in the presence of accompanying metals changes

Thesis tasks and time schedule:

No	Task description	Deadline
1.	Literature Review of previous research and relevant articles	20.04.2020
2.	Experimental analysis (limited)	20.05.2020
3.	Compilation of thesis report	25.05.2020

Language: English **Deadline for submission of thesis:** "....."".....2020

Student: …….. .....……..... "....."…….....2020

/signature/

Supervisor: …… …….. "....."".....2020

/signature/

Supervisor: …… …….. "....."".....2020

/signature/

Head of study programme: Karin Pachel "....."".....2020

/signature/

Terms of thesis closed defence and/or restricted access conditions to be formulated on the reverse side

Contents

List of Figures:

List of Tables:

Preface

Inorganic Scaling in Reverse Osmosis membrane filtration has been a major obstacle for its wide-scale implementation due to the additional incurred costs for cleaning and sometimes frequent replacement of membranes caused by it. The scaling process is complex in a sense that the chemical composition of the feed water is not homogenous, and research on the influence of the presence of trace elements on inorganic salt crystallization, and in turn the membrane scaling is limited. This led my supervisor at UCT Prague, Ing. Marek Šír to start working on determining the influence of metal ions in feed water on Calcium Sulphate/Gypsum scaling. This thesis is in concurrence to the previous work which was focussed on the influence of Iron (Fe). In our present study, '**Crystallization kinetics of Calcium Sulphate in the presence of metal ions**', we focussed on determining the influence of Zinc and Manganese ions on the crystallization of gypsum at various solution and ionic concentrations. Crystal morphology and elemental distribution studies were also carried out to substantiate the findings from the analysis of crystallization process.

I would like to take this opportunity to thank Almighty God for being able to complete my thesis in such crisis. I thank Ing. Marek Šír, PhD at UCT Prague for his indispensable guidance and mentorship throughout the course of project. I am also thankful to my supervisor Prof. Karin Pachel, PhD, Program Head, Environmental Engineering and Management, Tallinn University of Technology, for agreeing with the topic and providing support at every step with valuable inputs.

I am thankful to all the faculty members and administrative staff at TUT Tallinn, IST Lisbon and UCT Prague for their support all along the Erasmus mobility programs I took part during the two years of my Master's studies.

I would also like to thank all my colleagues and friends I made from all across the world for their presence and interactions that made my journey of Master's Degree cherishable.

Last but not least, I am grateful to my family, especially my mother and my father, who supported me throughout, and without whom I would not have reached this far in my life.

Keywords: Reverse Osmosis; membrane separation/filtration; membrane fouling; inorganic scaling; Calcium Sulphate (Gypsum); crystallization; super saturation; induction period/time; crystal morphology.

List of Abbreviations

1. OECD - Organisation for Economic co-operation and development countries
2. BRIC - Brazil, Russia, India China
3. ROW - Rest of the world
4. RO - Reverse osmosis
5. NF - Nanofiltration
6. UF - Ultrafiltration
7. MF - Microfiltration
8. PV- Pervaporation
9. ED - Electrodialysis
10. MD- Membrane distillation
11. SW - seawater
12. BW - brackish water
13. CDA - Cellulose diacetate
14. IDA - International Desalination Association
15. IS - Ionic Strength
16. BCS - brine conversion system
17. EPS - Extracellular Polymeric substances
18. NOM - Natural Organic Matter
19. TEP - Transparent Exopolymer particles
20. PA – Polyamide
21. O & M - Operation and Maintenance
22. SI - Saturation Index
23. IAP - Ion Activity Product
24. CP - Concentration Polarisation
25. SQL - Structured Query Language
26. SEM - Scanning Electron Microscopy
27. EDS - Energy Dispersion Spectrometer

Chapter 1: Introduction

One of major challenges in many countries around the world is water shortage. The world population has increased fourfold while the fresh water consumption has increased ninefold in the 20th century. By the year 2025, several countries are expected to face severe water crisis; the problem being manifold critical where water shortage already exists (Fig. 1) [1]. It is aggravated by water pollution from farming residues, domestic sewage as well as industrial waste. In order to meet the rising demand for fresh water, strategies like water reuse and seawater desalination have already been applied. Membrane technology is one of the most efficient technologies used in these strategies to produce high quality water [2].

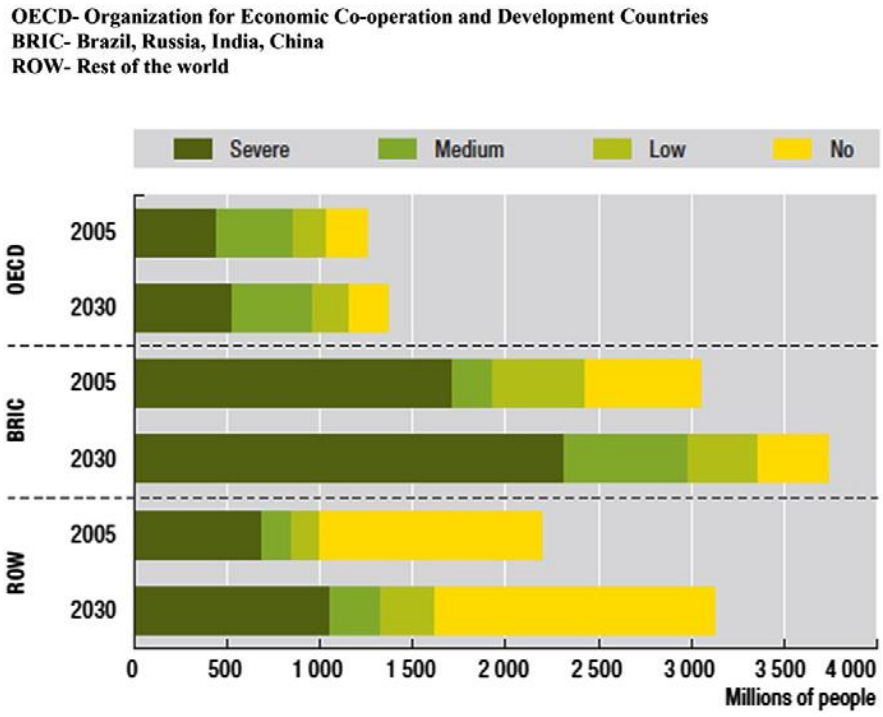

Figure 1: People living in areas of water stress, by level of stress, Source: OECD Environmental Outlook to 2030 [1]

1.1 *Membrane separation processes – History and classification*

Membrane separation processes have undergone rapid growth during the past few decades, especially due to the ever-increasing demand of fresh water for various domestic and industrial needs. Though the studies of membrane phenomena can be traced back to eighteenth century philosopher scientists, they had no industrial or commercial uses, but were used as laboratory tools to develop several physical and chemical theories. Few such instances include - the use of term 'osmosis' by Abbe Nollet to describe permeation of water through a diaphragm, 1748; development of Van't Hoff limit law, 1887. In 1907, Bechhold

devised a technique to prepare nitrocellulose membranes of graded pore size, which he determined by a bubble test and by the early 1930s, microporous collodion membranes were commercially available [3].

Membranes found their first significant application in the testing of drinking water at the end of World War II after several water supplies serving large communities in Germany and elsewhere in Europe had broken down, and filters for water treatment were needed urgently. By 1960, the elements of modern membrane science had been developed, but suffered from four main problems that prohibited their widespread use as separation process: they were too unreliable, too slow, too unselective, and too expensive. The seminal discovery that transformed membrane separation from a laboratory to an industrial process was the development, in the early 1960s, of the Loeb-Sourirajan process of making defect-free, high-flux, anisotropic reverse osmosis membranes form cellulose diacetate (CA). The period from 1960 to 1980 produced a significant change in the status of membrane technology. Building on the original Loeb-Sourirajan technique, other membrane formation processes including interfacial polymerization and multilayer composite casting and coating were developed for making high performance membranes [4].

The processes in which membranes are used can be classified according to the driving force used in the process. This driving force maybe difference in pressure, concentration, temperature, chemical potential and so on. The driving force along with the membrane permeability and membrane thickness determine the *flux* [3].

$$Flux = \frac{Membrane\ \ Permeability}{Membrane\ Thickness}(Driving\ force) \qquad (1)$$

Membranes for industrial separation can be broadly classified into the following four groups according to the driving force that causes the flow of permeate through the membranes:

1. Pressure-driven membrane process:
    - Reverse osmosis (RO)
    - Nanofiltration (NF)
    - Ultrafiltration (UF)
    - Microfiltration (MF)
    - Pervaporation (PV)
    - Membrane gas separation
2. Concentration gradient driven membrane process:

- Dialysis
- Membrane extraction

3. Electrical potential driven membrane process:
    - Electrodialysis (ED)
4. Temperature difference process:
    - Membrane distillation (MD)

Table 1: Classification of Membrane separation processes – based on driving force

Driving Force	Membrane Process	Permeate	Retenate	Type Of Membrane
Pressure Difference	Reverse Osmosis (10 - 100 bar)	water, small polar solvents, salts	all solutes, water	assymetric skin type
	Nanofiltration (10 - 70 bar)	Monovalent ions, water	Small molecules, divalent salts	Thin-film membranes
	Ultrafiltration (1 - 10 bar)	Small molecules, water	Polymers, proteins, micelles, colloid particulates	Asymetric microporous
	Microfiltration (0.5 - 2 bar) Gas seperation	Dissolved solutes, water gases ($\preceq 1$ nm) and polar vapours	Suspended particles, water gases	Symmetric microporous, Asymetric homogenous polymer
	Pervaporation	Volatile small molecules, water	Low volatility species; species less soluble in the membrane	Asymetric homogenous polymer (a nonporous membrane)
Concentration difference	Dialyss membrane extraction	Small molecules, water gases, solutes, vapours soluble in the extractant	Large molecules, water components of feed insoluble in extractant	Nonporous or microporous
Electrical potential difference	Electrodialysis	ionized solutes, water	Non ionic solutes, water	Ion exchange membrane
Temperature difference	Membrane distillation		Molecules, < 1nm	Microporous

Apart from above processes, there are other membrane processes such as facilitated or carrier mediated membrane transport, liquid membrane separation, pertraction, membrane contactors, membrane reactors, charge mosaic membranes, and piezo dialysis and hybrid processes in which membrane separation is combined with conventional processes [3].

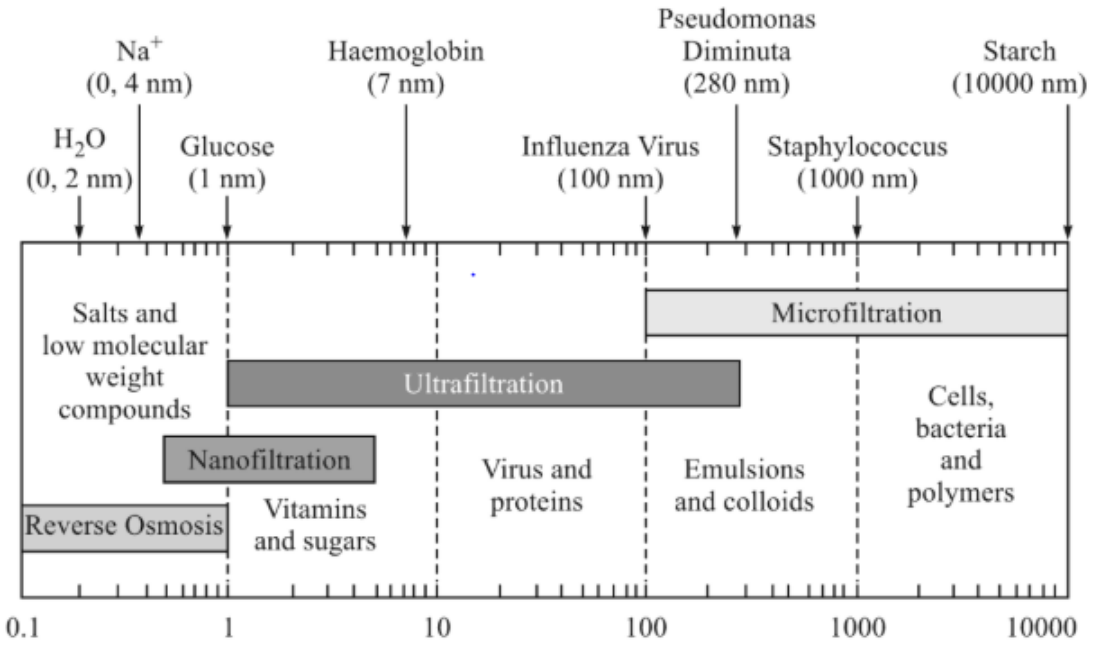

Figure 2: The relative size of different solutes represented against the pore diameters of various filtration membranes [3]

1.2 ***Reverse Osmosis (RO) – advantages and drawbacks***

All the aforementioned membrane technologies are used to various degrees in desalination of water, both seawater (SW) and brackish water (BW). The International Desalination Association (IDA) reports that 18,426 desalination plants were operated worldwide until June 2015 that could provide about 87 million cubic meters of water for 300 million people daily usages. Till the end of 2017, the total desalination capacity all over the word has reached almost one hundred million m^3/d. Particularly, RO desalination has advanced significantly in the last few decades and dominated the desalination area. For instance, in 2017 the newly-built membrane-based desalination capacity was 2.2 million m^3/d while that of thermal-based was only 0.1 million m^3/d. Nowadays, RO desalination accounts for>60% of the total desalination around the world [5].

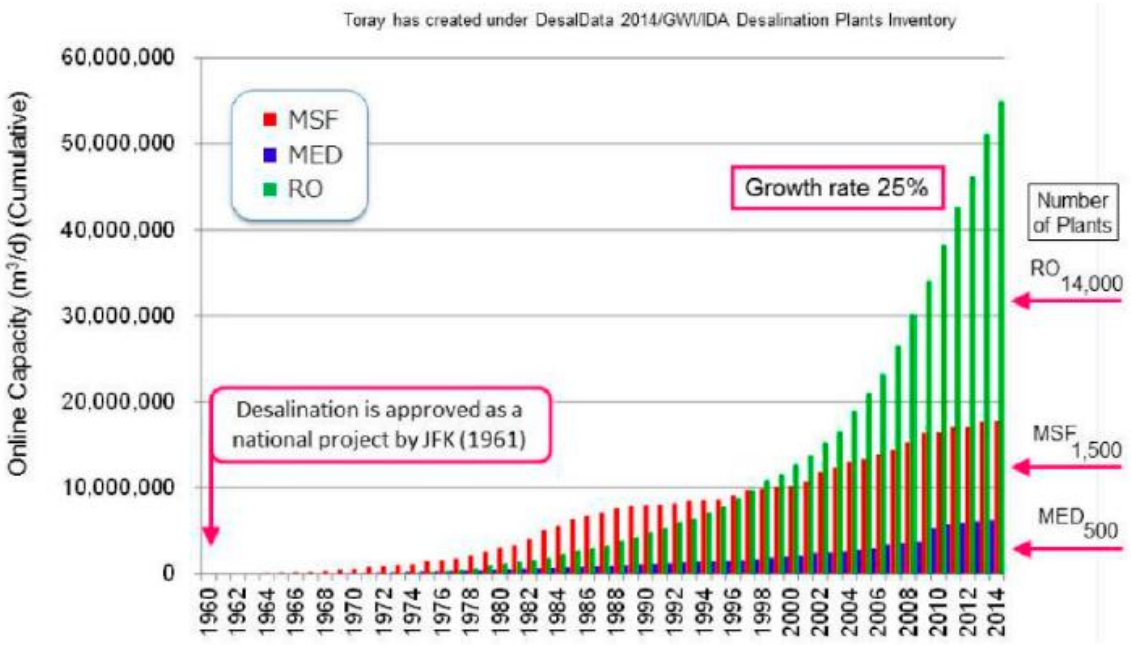

Figure 3: Online capacity of various desalination technologies and the expansion of the global desalination market [7]

Separation technologies are more concentrated about energy usages, sustainability, and environmental issues [5]. Initially, the desalination plants relied on thermal distillation processes, but after the 1980s, those were replaced with more efficient and economic RO technology. Osmosis is a natural process that occurs between two fluids separated by a semi-permeable membrane that allows passage of the solvent (e.g., water) but slows down the passage of dissolved solids. The direction of the water flow is determined by the pressure, temperature and concentration of dissolved solids [6]. The energy requirement for RO processes was further lowered via extensive research in desalination practices. The development of superior membrane materials, energy efficient variable speed high pressure pumps and motors, and energy recovery devices have significantly lowered the energy requirement of this process. In comparison to the 1970s, the energy footprint of RO processes has decreased from 20 kWh/ m^3 to less than 2 kWh/ m^3 at this moment for seawater desalination and about 1 kWh/ m^3 for brackish water desalination [7] [8]. treatment. RO is currently the most energy-efficient technology for desalination, with average energy cost about 1.8 kWh/ m^3, which is much lower than that of other technologies and hence very widely used [2] [9] [10].

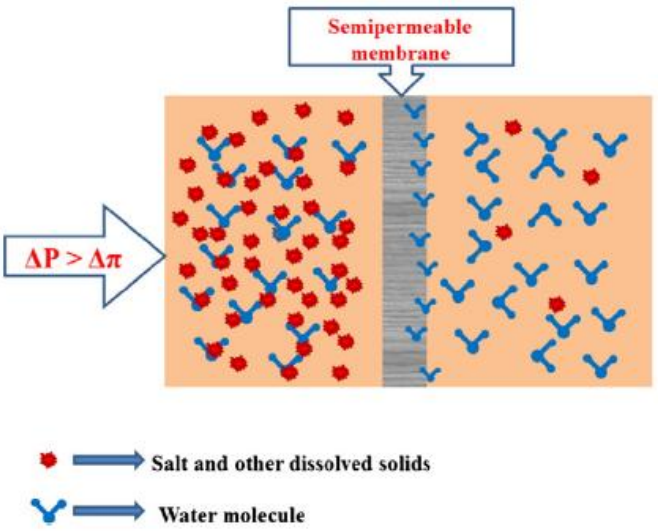

Figure 4: Schematic illustration of Reverse Osmosis process [1]

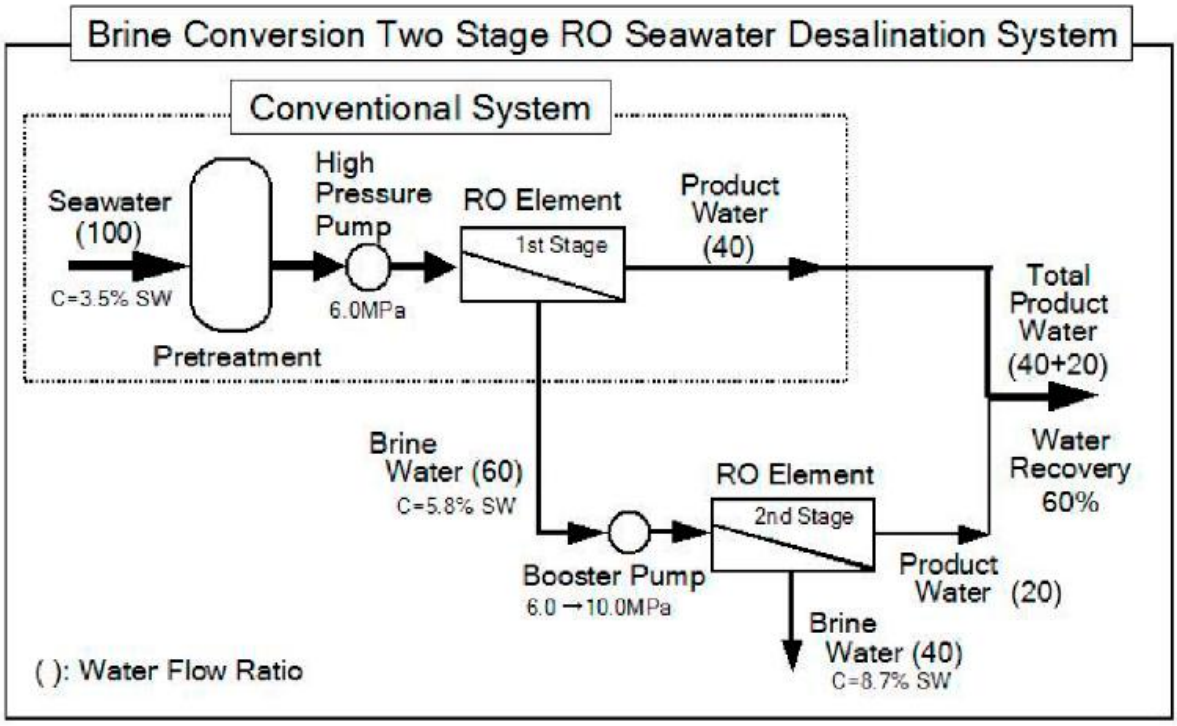

Figure 5: Two-stage Brine conversion system (BCS) [11]

However, RO membrane fouling is a main challenge to reliable membrane performance [2] [12]. In order to mitigate the inborn fouling issue which is specific to membrane-based desalination, numerous approaches have been established and published in the literature. These strategies involve the surface modification and development of novel desalination membranes, pre-treatment, and cleaning as well as monitoring and optimisation of operating conditions [9]. Membrane fouling could significantly reduce productivity and permeate quality while increasing operation cost due to increased energy demand, additional pre-

treatment, foulants removal and membrane cleaning, maintenance, as well as reduction in membrane lifetime [13] [14] [15].

1.3 ***Membrane fouling – influencing factors and types***

The fouling of pressure-driven membranes is generally referred to the accumulation, deposition, and/or adsorption of foulants onto the surface of membrane and/or within the membrane pores, which can cause the basic membrane functions to deteriorate over filtration time, including permeate flow, solute removal efficiency, and pressure drop across the membrane [2] [10]. The factors affecting the membrane fouling are as follows [16] [17]:

Membrane properties: In an aqueous environment, a membrane can be attractive or repulsive to water. The composition of the membrane and its corresponding surface chemistry determine its interaction with water, thus affecting its wettability. Hydrophilic membranes are characterized by the presence of functional groups that have the ability to form hydrogen bonds with water and so these membranes are highly wetted by water [17]. Hydrophobic membranes have the opposite interaction to water compared with hydrophilic membranes as they have little or no tendency to adsorb water and water tends to form beads on their surfaces (i.e., discrete droplets). This tends to enhance fouling. Particles, which foul membranes in aqueous media, tend to be hydrophobic and cluster or group together to form colloidal particles because this process lowers the interfacial free energy [17]. Thus, fouling can be reduced with use of membranes with surface chemistry which have been modified to render them hydrophilic [17]. It is hence clear that the membrane surface properties are one of the most important factors to influence surface fouling of RO membranes. Among others, surface roughness, hydrophilicity, and electrostatic charge are identified as the three most important surface properties [18].

Solution properties: The properties of the feed solution also significantly influence membrane fouling. Some of the important feed properties are solid (particle) concentration, particle properties, pH, and ionic strength (IS) [17]. In general, an increase in the feed concentration results in a decline in the permeate flux, which is due to the increase in membrane fouling by the presence of a higher foulant concentration. Particles may be present in the feed because of the nature of the feed or through precipitation of soluble feed component(s) [17]. The particles can cause fouling by pore blocking, pore narrowing, or cake formation, depending on the particle sizes [17]. Some other factors, such as pH, IS, and

electric charges of particles, are also important because these factors affect the interaction forces working between the particles and thus affect the particle agglomeration.

Operating conditions: The RO operating conditions also affect fouling. Increase in feed flow velocity decreases the concentrated layer thickness. Changing the feed temperature from 20°C to 40°C led to an increase in the permeate flux up to 60% [19]. This might be due to the fact that changes in the feed water temperature resulted in changes in the permeate diffusion rate through the membrane [17].

Fouling can be divided into surface fouling and internal fouling, in terms of the fouling places [2]. Depending on the nature of foulants, the fouling of RO membrane can be classified into scaling (inorganic fouling), bio fouling, organic fouling, and colloidal fouling [2] [16]. Also, there is another classification with chemical oxidation by residual chlorine replacing the colloidal fouling [10] [20].

I. Scaling

Generally, scaling refers to the inorganic fouling which is caused by the precipitation or crystallisation of inorganic minerals ions such as calcium, magnesium, carbonate, sulphate, and phosphate [10] [21]. As the solubility of some inorganic scalants is pretty small or the concentration of some ions in the water is pretty high, when they exceed the equilibrium solubility product and become supersaturated, they will deposit on the surface or the pores of the membrane, resulting in scaling [2] [22]. Scale formation involves the complex mechanisms of both crystallisation and transport process [10]. The principle stages of scaling in RO membrane systems are illustrated in Fig. 6 [23].

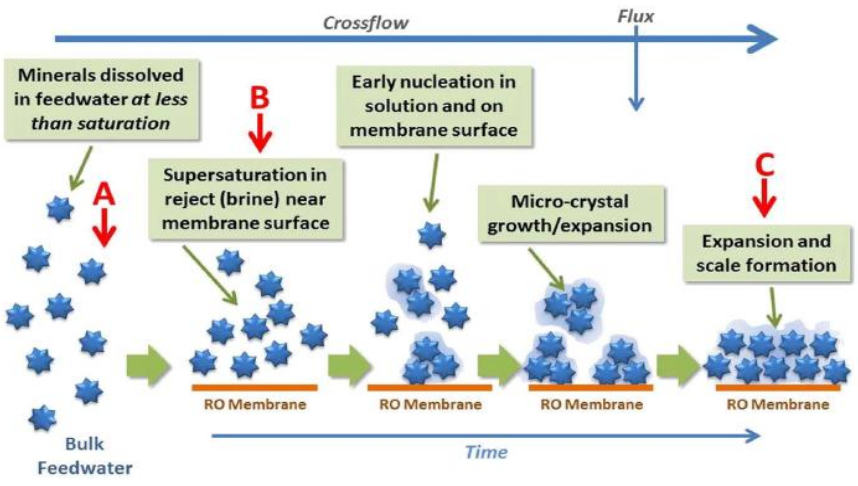

Figure 6: Schematic illustration of the key steps in scale formation onto RO membrane surface over time [23]

II. *Bio fouling*

Biofouling is the process of microorganism adhesion and proliferation on membrane surface. In other words, it is the formation of biofilm to an unacceptable degree which could cause huge operational costs. Biofilm formation is essential in this process [2] [24]. Biofouling is more complex than other fouling types. There are two key components of biofilms, namely the bacteria and the extracellular polymeric substances (EPS) which are excreted by bacteria during the metabolism process [2] [25]. According to Flemming (1997) [77], biofilm development could undergo three stages, namely induction, logarithmical growth and plateau stages. From another perspective, biofilm formation could be briefly divided into three phases in terms of bacteria activity and mobility, and the three phases are bacteria attachment, reproduction, and detachment [2]. For a biofilm to form, two conditions are essential, namely the presence of bacteria as well as the nutrients. So, the logic is that if all the nutrients are removed from the water through pre-treatment technologies, then the remaining cells could not proliferate due to lack of food sources. Other factors that affect this process are listed in Fig. 6 [2].

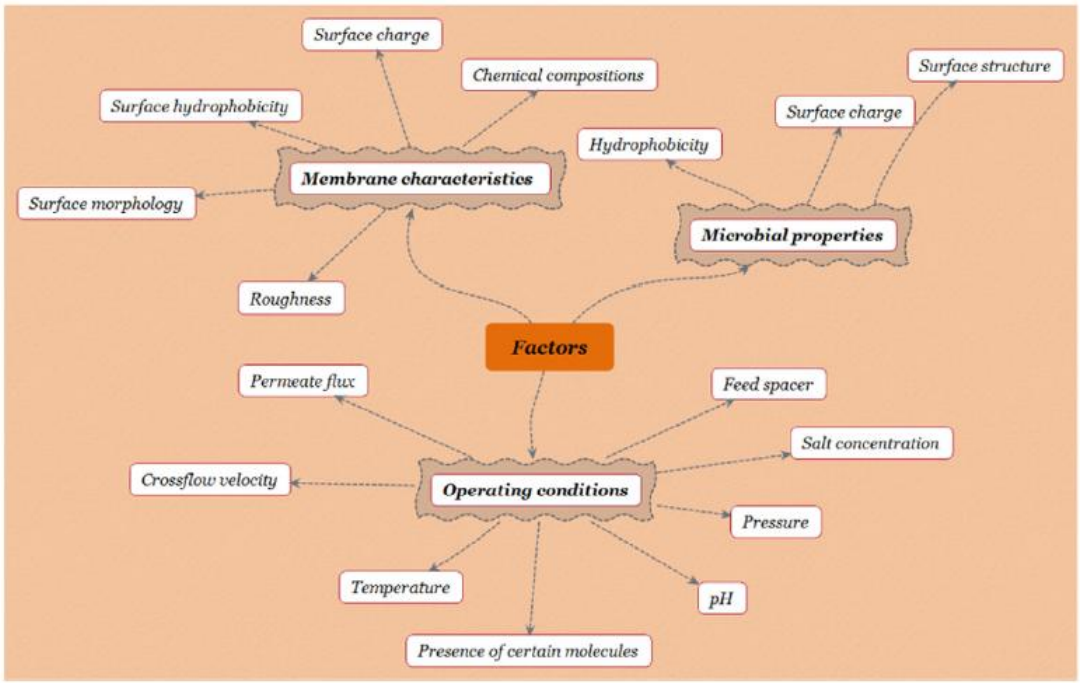

Figure 7: Factors affecting bacteria attachment to membrane surface [2]

III. *Organic fouling*

Organic fouling is the combination of deposition, reactions, and interactions of high-molecular-weight organic molecules, e.g., Natural Organic Matters (NOMs) and/or

Transparent Exopolymer Particles (TEPs) with the membrane surface [10]. In different situations the influence of various organic matter on RO fouling could be different, as in one kind of organic matter can be the primary foulant in one situation but replaced by another organic foulant in a different situation. It can however be concluded that the three important factors influencing organic fouling are feed water chemistry, foulant-surface interactions as well as foulant–foulant interactions [2]. Organic fouling is hard to eliminate due to the complex structures formed by dissolved organic matters in combination with other substances and could result in significant flux decline of RO membranes and it [2] [26] [27] [28]. The molecular weight of organic matters is another important factor for membrane fouling [2] [29]. Moreover, pre-treatment technologies like coagulation can remove organic matters with high molecular weight easily in comparison to organic matters with a low molecular weight which are more difficult to be removed [2] [30].

IV. Colloidal fouling

Colloids are fine suspended particles, the size of which ranges from a few nanometres to a few micro meters, although some references state that the size of colloids ranges from 1 nanometre to 1 micrometre [2] [31] [32]. Colloidal fouling refers to fouling of the membrane caused by the colloids or particles depositing on the host materials [2] [33]. The common colloidal foulants can be divided into two types, i.e., inorganic foulants and organic macromolecules. The major inorganic foulants in nature water include aluminium silicate minerals, silica, iron oxides/hydroxides while the organic macromolecules in the water are mainly consisted of materials such as polysaccharides, proteins, as well as some natural organic matters [2] [34]. Feedwater characteristics such as the concentrations of the foulants and the physiochemical characteristics, membranes properties as well as operational conditions, could also be impact the formation of a colloidal cake layer similar to other types of fouling [2] [35] [36] [37] [38].

V. Chemical oxidation by residual chlorine

Oxidising agents like chlorine species are commonly added into the RO feed stream as water disinfectants and bactericides for biofouling control of direct media filtration systems [39]. Even though the feed water is dechlorinated prior to the membrane system, the exposure to very low concentration of residual chlorine still occurs [20]. Chlorine in the form of hypochlorous acid (HOCl) and hypochlorite ion (OCl^-) attack the PA top dense layer, causing the occurrence of N-chlorination by substituting the hydrogen on amide nitrogen

firstly, followed by ring-chlorination via an intermolecular rearrangement called Orton rearrangement [40], as shown in Fig. 8. As a result, the degradation of PA layer takes place and then leads to the loss of membrane integrity and eventually causes an increase in membrane flux and salt passage [10].

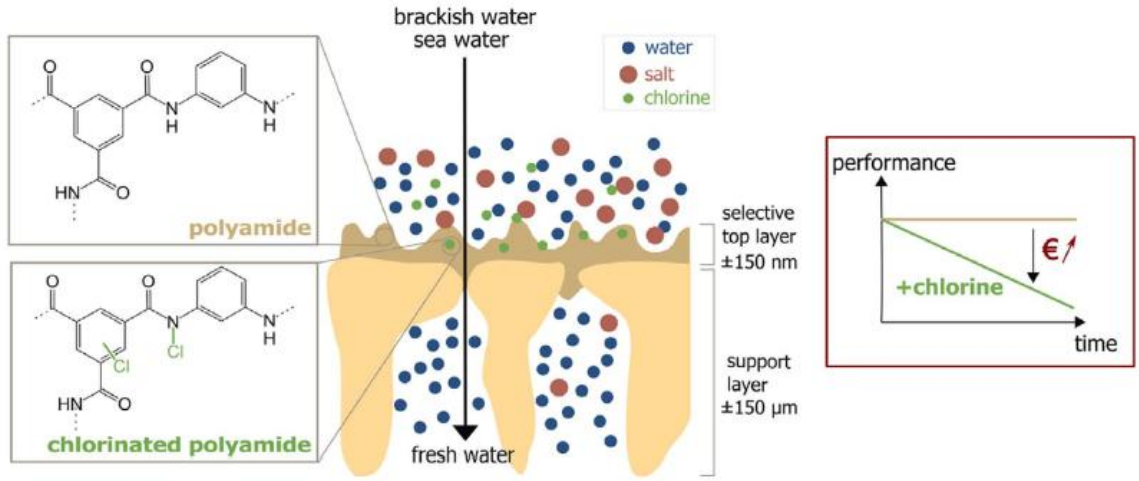

Figure 8: Schematic diagram of chlorine attack on PA membrane and the performance decline due to the attack [20]

1.4 Control Strategies of Inorganic Scaling

Due to the significance importance on the performance and efficiency of the membrane module and hence, on the overall economics of the process, control of scale formation is of utmost importance. The majority of scale control routes fall under one of the following categories: (i) feed water pre-treatment to lower its scaling potential, (ii) adjustment of operational conditions, (iii) membrane modification [2] [10] [41].

Pre-treatment – The main objective of installing pre-treatment facilities is to improve the quality of raw feed water to ensure reliable RO operation and as well as prolong RO membrane lifespan by reducing scaling. Pre-treatment methods could be selected based on the source water composition analysis. For example, for feedwater that has a high hardness level, pre-treatment to reduce hardness is necessary so as to reduce membrane scaling risk. Years [2]. As shown in Fig. 9, UF, coagulation/flocculation and MF are the three technologies that have been most studied by researchers as RO pre-treatment methods [2].

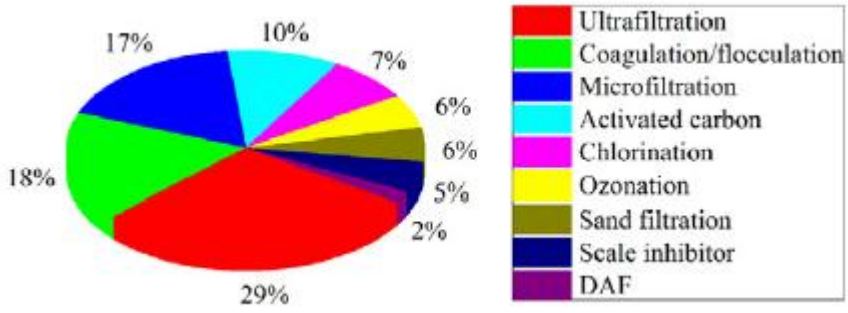

Figure 9: Common studied RO pre-treatment technologies in the past 10 years [2]

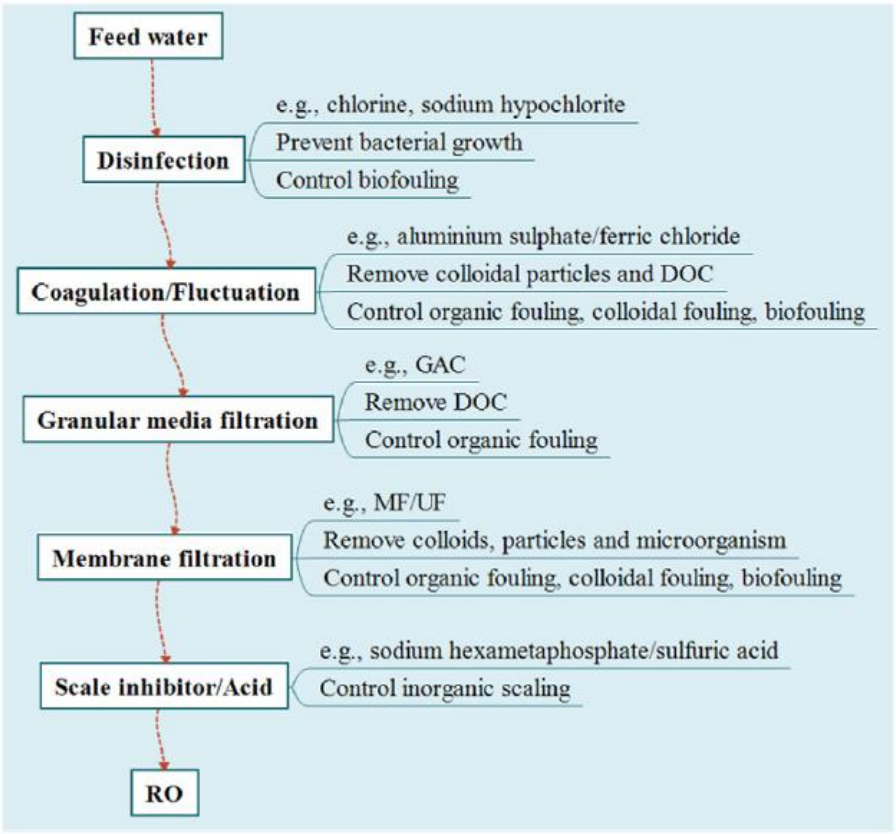

Figure 10: Schematic diagram of RO pre-treatment processes and their roles in fouling control [2]

Adjustment of Operational conditions - Besides membrane feed pre-treatment, optimisation of operational conditions within the design limitations of different RO modules is also crucial to control the fouling. Operational conditions such as temperature, applied hydraulic pressure, pH, and hydrodynamic condition can be manipulated to suppress the fouling development [10].

i. Temperature - It has a significant impact on the separation performance and membrane fouling in RO. Separation performance is improved at high temperature as the salt diffusivity increases due to low solution viscosity as well as membrane

network pore swelling, hence increasing the permeate flux. However, elevated temperature affects the fouling formation on the membrane surface [10].

ii. Pressure - Membrane fouling is also strongly dependent on applied pressure. Higher applied pressure would result in higher initial flux hence promoting the fouling development. The increase in applied pressure would increase the polarisation layer thickness and concentration in the membrane, thus increasing the concentration polarisation and fouling development [42].

iii. pH - Studies on the effect of pH on membrane fouling are also important as pH affects the electrostatic interactions of foulant molecules. However, at high ionic strength as that of seawater, the effect of pH is not significant because the overall charge density of organic macromolecules is completely masked, which supersedes the effect of protonation of organic functional groups. Therefore, it could be suggested that the pH is not a dominant factor in determining the organic fouling rate in seawater desalination [10].

iv. Hydrodynamic conditions - Many studies have emphasised the importance of hydrodynamic conditions on the development of membrane fouling. It is crucial to manipulate the hydrodynamic conditions such as cross-flow velocity and flux to improve the membrane filtration process. In general, membrane fouling can be reduced at high cross-flow velocity and/or low flux. High cross-flow velocity induces high shear rates which promotes the back diffusion of particles away from the membrane surface and reduces the concentration polarisation, thus minimising fouling development [43] [44].

Membrane modification - Membrane fouling in RO systems is closely related to surface characteristics [2] [45]. Among these characteristics, surface smoothness and hydrophilicity are reported to be two important factors affecting membrane fouling [2]. Membranes with smooth and hydrophilic surfaces demonstrated less fouling tendency than those with rough and hydrophobic surfaces [2]. As shown in Fig. 11, membrane (a) and (c) have hydrophilic surfaces while membrane (b) and (d) have hydrophobic surfaces. Meanwhile, membrane (a) and (b) have smooth surfaces while membrane (c) and (d) have rough surfaces. Therefore, membrane (a) is expected to have the best anti-fouling performance while membrane (d) is the worst. A layer of water could be easily formed on a hydrophilic surface and foulants with hydrophobic property are repellent to the surface. But it should be clarified that in certain

situations hydrophilic membranes are more inclined to attract hydrophilic substances and thus induce fouling [2] [46].

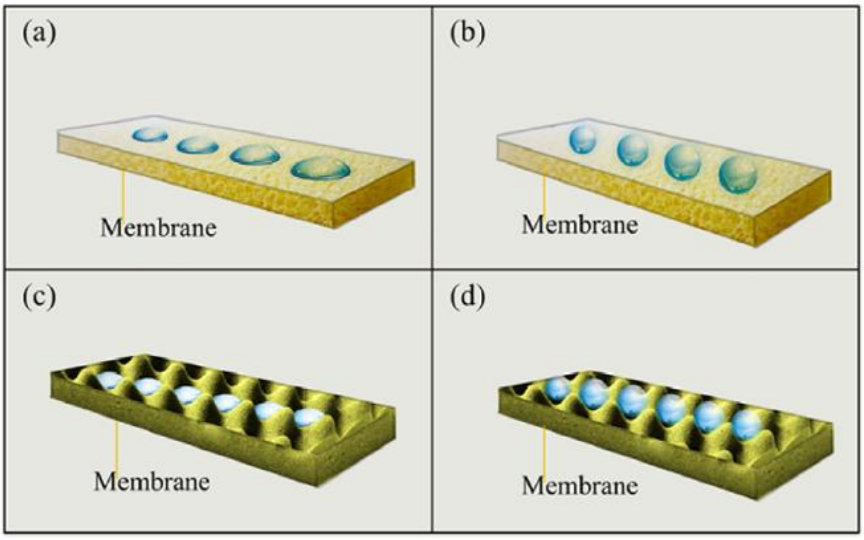

Figure 11: Schematic diagram of membrane surface smoothness and hydrophilicity [2]

The main aim of surface modification is to alter the surface properties like surface charge, morphology, hydrophilicity and chemical groups of a membrane, to facilitate fouling resistance. Many studies have been conducted about membrane surface modification, of which majority only focused on certain types of foulants, and thus their applications would be greatly limited. Though the fouling resistance was enhanced through modifying membrane surfaces, there might be negative effects on membrane performance, such as decreased water flux [2].

1.5 Inorganic Scaling – significance

In this study we mainly focus on understanding the Inorganic scaling by gypsum and the crystallization kinetics involved. Mineral salts such as $CaCO_3$, $CaSO_4$, and $BaSO_4$ are almost always present near their saturation levels in brackish water feeds. Therefore, even at moderate levels of product water recovery, there is a good likelihood of inorganic fouling taking place [47]. An extraction of even small volume of water will most probably raise the concentration level of these sparingly soluble salts to exceed their solubility limit [48]. Hence, precipitation will occur with salt crystals either forming directly on the membrane surface or in the bulk. The deposition will lead to a decline in permeate flux and a shorter membrane life [49]. Therefore, it is difficult to achieve high product water recovery for sources with high scaling potential [41]. The crystals of the precipitated salts accumulate on the membrane and related components such as feed and permeate spacers resulting in

permeate flux decline and an increase in pressure drop across the element [50]. Furthermore, the removal of foulants necessitates chemical cleaning that may damage the membranes and shorten their service life [51]. Therefore, as a result of inorganic fouling, the operation and maintenance (O & M) cost of an RO plant increases due to higher consumption of energy [52], system downtime [53], necessary membrane area [54], and expenses of membrane cleaning [24].

Statistical analysis revealed that in the last 25 years, over 3000 papers were published to address the issue of RO membrane fouling (shown in Fig. 12), indicating researchers' great interest in this area [2]. Based on this model, and assuming that no revolutionary breakthroughs in RO membrane technology and alternative technologies as well will be made in the next ten years, then it can be predicted that by the year 2022, the cumulative number of papers published will possibly be about twice that of 2016. Although the research trend may not be predicted precisely simply by this model, it can at least give us an indication that research interest in this field will continue to bloom [2].

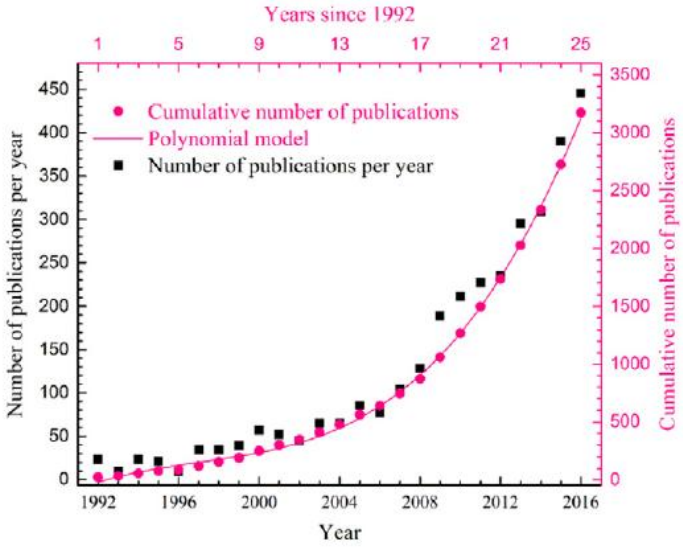

Figure 12: Number of publications per year and cumulative number of publications on RO fouling over the past 25 years [2]

Statistical analysis also revealed that calcium carbonate and calcium sulphate were the most studied inorganic scalants by researchers in the past 10 years, which is indicative of their dominant role in causing inorganic scaling in RO(shown in Fig. 13) [2]. Different ions may have different effects during the scaling process. The factors that govern the mechanism of precipitation and dissolution of these sulphate salts are therefore of considerable interest, especially the degree of saturation, ionic strength, temperature and the influence of foreign

cations which may exert a marked effect on the rates of precipitation and dissolution [55]. Basically, the compositions of salt deposits on RO membranes are determined by inorganic compositions in feedwater, chemicals added during pre-treatment, as well as the chemical properties of the sparingly soluble inorganic salts [2] [56]. Hence, our study dealing with the influence of metal ions on the process of crystallization of $CaSO_4$ that in turn affects the scaling phenomena on the membrane surface, is one of the important aspects to be studied in order to improve the overall efficiency of the process and increase the membrane lifespan.

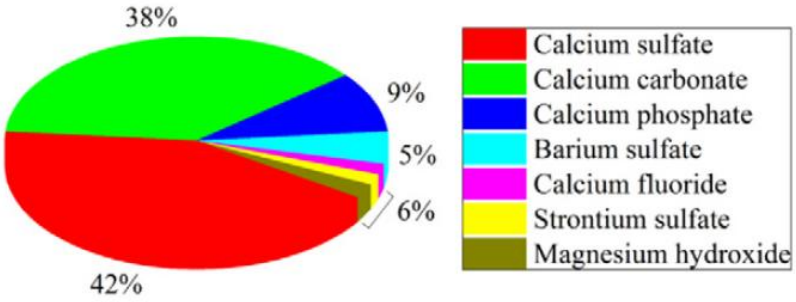

Figure 13: Common studied inorganic foulants for RO in the past 10 years [2]

1.6 $CaSO_4$ - Crystallization kinetics

Scale formation is known to occur by two crystallization routes (a) bulk crystallization (homogeneous nucleation), where the salt precipitates in the solution and (b) surface crystallization (heterogeneous nucleation), when the crystals form on the membrane surface [5] [41]. The major difference between these two types is that in the former, crystals form in the bulk solution and are then transported to the membrane surface by convection, while, the formation of salt crystals and their subsequent growth occur at the membrane surface in the latter [57]. Typically, the latter is energetically more favourable and hence, more frequent for lower levels of supersaturation. However, it should be noted that bulk nucleation and/or crystallization is not necessarily homogeneous as it could occur on a suspended solid far away from the membrane surface. The existence or prevalence of one mechanism over the other seems to depend upon several diverse factors such as (i) degree of local supersaturation, (ii) hydrodynamics, (iii) feedwater temperature and pH, (iv) presence of other foulant types e.g. organic matter. Also, it is worth mentioning that experiments performed in laboratory-scale units have their own limitations due to relatively smaller membrane area and limited recovery of permeate water (> 10%) [41].

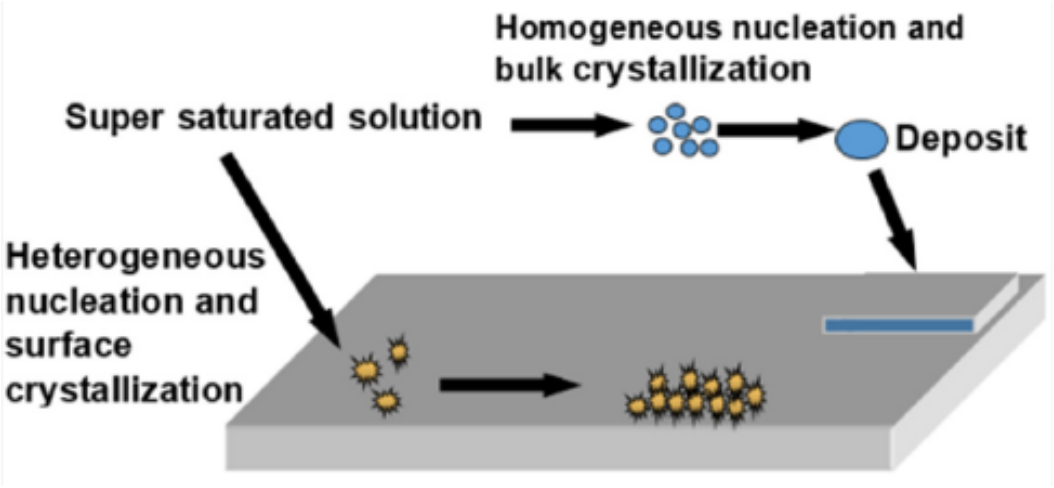

Figure 14: location of nuclei and crystals formation for both homogeneous and heterogeneous processes [41]

The following are the sequence of events leading to scaling:

a) *Supersaturation & Aggregation*: In a solution, collisions of oppositely charged ionic species are occurring continuously and there is a dynamic equilibrium between the formation of ion pairs and their dissociation. However, once supersaturation is achieved for a certain compound, the ion pairs become more stable and have a less tendency to dissociate. When a large no. of such pairs come together, they form micro-aggregates that act as centers of crystals or seeds [58]. The extent of supersaturation for a particular salt can be expressed with respect to the activity of the ions making up the salt and the solubility product in the equation given below:

$$SI = \log\left[\frac{IAP}{K_{sp}}\right] \qquad (2)$$

Where,

SI = Saturation Index

IAP = Ion Activity Product and

K_{sp} = Solubility Product

The ion activity product is a combination of the activity coefficient and the concentration of both ions (e.g. Ca^{2+} and SO_4^{2-}) making up the salt. The solubility product constant, K_{sp}, is the equilibrium constant for a solid substance dissolving in an aqueous solution and represent the level at which a solute dissolves in solution. The solubility product for the above reaction will be simply the product of the concentrations of the component ions i.e. $K_{sp} = [Ca^{2+}]\cdot[SO_4^{2-}]$. When the ratio IAP/K_{sp} is > 1, there is a high probability of salt precipitation and hence, mineral scale formation [41].

b) *Nucleation*: In this stage, micro-crystals are formed around the micro-aggregates that act as nucleation centers for crystallization. Nucleation is of two kinds: if the supersaturation is very high wherein it may take place in the fluid bulk (homogeneous) [59], or as is usually the case occurs on a substrate (heterogeneous) [60]. The nucleation rate can be expressed as a function of free energy change [41]:

$$J = Aexp\left(\frac{-\Delta G_c}{kT}\right) \quad (3)$$

Where,

k = Concentration Polarisation (CP) coefficient

A = preexponential factor with a value of 10^{30} nuclei/cm^{3}s.

T = Temperature in Kelvin

ΔG_c = free energy change for the critical cluster size

$$\Delta G_c = \frac{16\pi\gamma^3 v^2}{3(kTSI)^2} \quad (4)$$

Where,

γ = the interfacial energy (mJ/m2) between the solid phases forming the liquid,

v = the molecular volume of crystals,

SI = Saturation Index,

T = temperature in Kelvin.

A very important parameter in the overall process of scale formation is the induction time that is defined as the time between the occurrence of supersaturation to the formation of stable nuclei of the precipitating salt [61]. In addition to the extent of supersaturation, this time is also influenced by the level of agitation, the viscosity of the solution and presences of impurities [62]. For homogeneous nucleation, the induction time is related to the SI in the following manner:

$$\log t_{ind} = A + \frac{B}{T^3 SI^2} \quad (5)$$

$$B = \frac{\beta\gamma V_m^2 NAf(\theta)}{(1.3R)^3} \quad (6)$$

Where,

R = the molar gas constant (J/mol.K),

NA = Avogadro's constant (mol-1),

$f(\theta)$ = correction factor depending on the type of nucleation,

β = geometric factor of 16π3 for spherical shape crystal.

c) *Crystal growth around the nucleus*: Once the nuclei become stable, they begin to grow by the incorporation of further ionic pairs. The nuclei grow to form microcrystals in a solution that agglomerate to form macro crystals, which have a tendency to adhere to the membrane surface [41].

d) *The growth of small crystals into larger ones*: Once adsorbed on the surface, the macro crystals grow in the lateral direction as active sites are present on the membrane surface. In this stage, the coverage and thickness of the foulant layer increases the extent of which depends on both the number of crystals nucleating on the membrane surface and their growth rate [63].

Calcium sulphate exists in three different forms depending on the hydration state: gypsum ($CaSO_4 \cdot 2H_2O$), hemihydrate ($CaSO_4 \cdot 0.5H_2O$), and anhydride ($CaSO_4$). Calcium sulphate (in the form of gypsum) is by far the most common and non-alkaline mineral salt that causes scaling in desalination of brackish water [41]. To complicate things further, it is also the most problematic as it cannot be controlled by pH adjustments of the feed solution [64]. Like other scaling types, gypsum has been found to be influenced by both surface and bulk crystallization [65]. The most thermodynamically stable phase at ambient temperatures and up to 40 °C is gypsum, which also has the lowest solubility, although interconversion between the phases takes place under different conditions [66]. The solubility of gypsum initially increases with temperature up to ~50 °C and then decreases. However, for the other two states, the solubility continuously decreases with increasing temperature beyond 20 °C and is more rapid for the hemihydrate (Fig. 15).

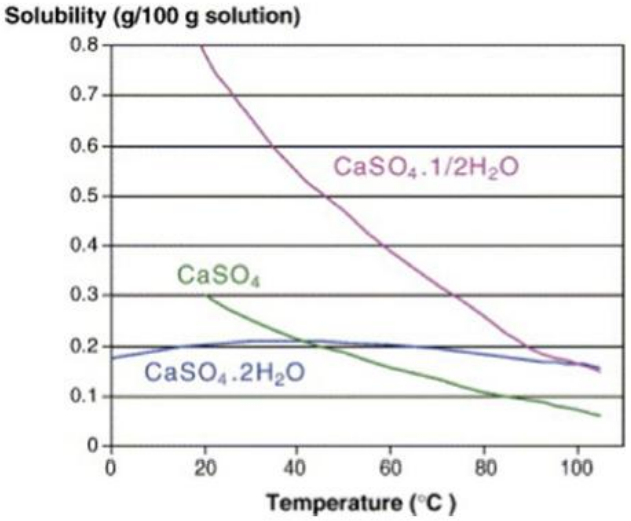

Figure 15: Variation of solubility with temperature for the different states of Calcium sulphate [67]

Due to its overwhelming importance and the hypothesis that gypsum probably does not form directly from solution, there has been recent renewed interest in the mechanisms of nucleation and growth [41]. Several studies have been directed towards a better understanding of $CaSO_4$ scale formation on membranes. In spite of the presence of many relevant studies, there still exists some controversy regarding the dominant scaling mechanism in actual situations and aspects such as the size of crystals, surface coverage, and affinity of the membrane for nucleation. Several studies have been performed to understand the underlying mechanisms of CaSO4 fouling. The observations strongly suggest the surface and not bulk crystallization to be the dominant mechanism in scaling by gypsum [13] [68]. Like its carbonate counterpart, calcium sulphate crystals may have different morphologies depending upon the conditions (Fig. 16). In the absence of scale inhibitors and ambient temperature and pressure conditions, the precipitating crystals are of regular rhombohedron shapes or rods depending on the solution concentration of Calcium and Sulphate ions (Fig. 16-a). On the other hand, the presence of anti-scalants will result in different morphologies such as needles, and plates. The crystal shape will be determined by the inhibition mechanism and its effectiveness in delaying precipitation onset [41].

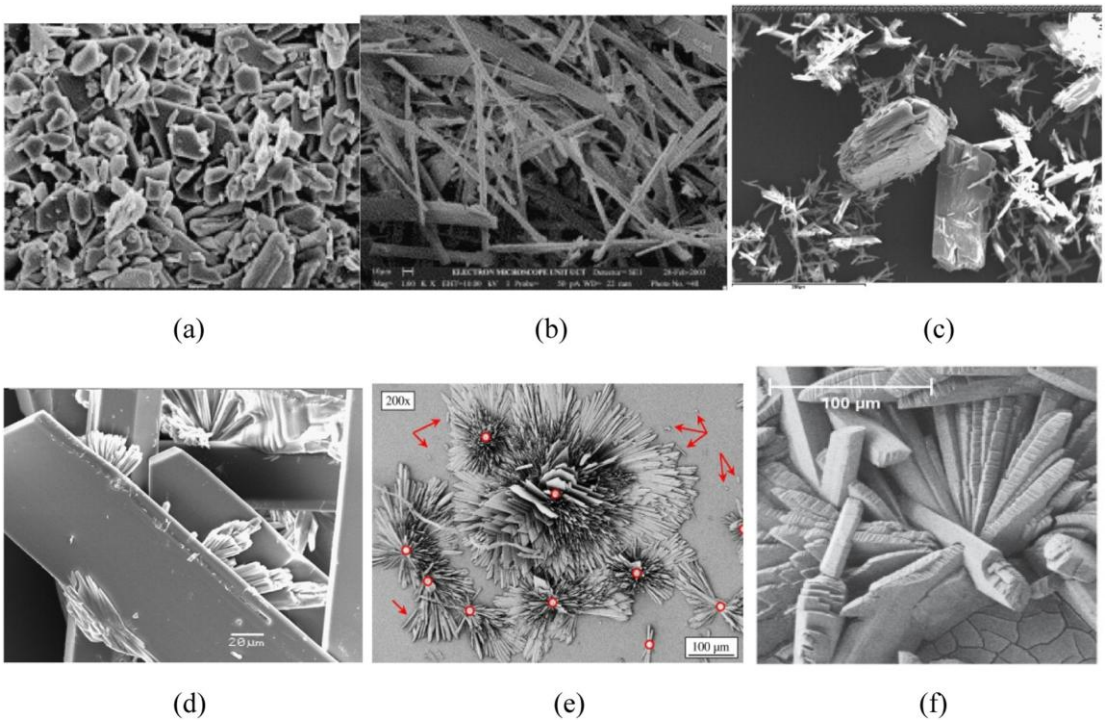

Figure 16: SEM images of surface covered with mineral scales of CaSO4 with different morphologies (a) rhombohedron grains [69] (b) stick-shaped crystals [69] (c) needle-like [70], and (d) distorted structure [70] (e) rosette-like [71] (f) rhombohedral

As mentioned before, extensive research has been carried out on the influence of physical parameters such as pH, temperature, pressure and turbidity, and the chemical additives like anti-scalants on the Calcium Sulphate dihydrate (Gypsum) scaling. But, through out very little emphasis was laid on the influence of trace metals. This is where our work focuses on filling this gap by studying the influence of metal ion concentrations on gypsum membrane scaling. Substantial studies providing enough evidence of the influence of metals like Iron (Fe), Chromium (Cr), Magnesium (Mg), Copper (Cu) and Cadmium (Cu) [73] [74] have already been carried out. They show how important the role of these metal ions is in inhibiting the crystallization process and thus prolonging the membrane lifespan. In our study we consider Zinc and Manganese to be the interest of study due to their considerable concentration in the feed water [75].

Chapter 2: Materials and methods

2.1 List of Chemicals used

From *Penta Chemicals*, Czech Republic:

a) Calcium Chloride ($CaCl_2$)
b) Sodium Sulphate (Na_2SO_4)
c) Zinc Chloride ($ZnCl_2$)

From *Carl Roth Chemicals,* Germany:

a) Manganese (II) Chloride monohydrate ($MnCl_2.H_2O$)

2.2 List of devices and software used

a) Tall form 250ml glass beakers
b) 1000 ml and 500 ml Volumetric flasks
c) WiseStir MSH-D Hotplate Magnetic stirrer, Witeg – Germany
d) Greisinger GMH 3430 conductivity meter, Germany
e) Adventurer Pro AV264C Analytical Balance, OHAUS – USA
f) Software Greisinger EBS 20M – to record the conductivity and temperature over time. The Greisinger EBS 20M is Software for 20-Channel Measurement Data Logging. The software enables the structure of a cheap and convenient multi-channel measurement data acquisition system. The program is ideal for recording, monitoring and documenting. This text is machine translated.
g) *Principle of conductivity*: Electrical Conductivity is a measure of the ability of a substance/solution to conduct an Electric Current (this electric current is carried by ions and the chemical changes that occur in the solution).
h) Scanning Electron Microscopy (SEM, Tescan VEGA 3-LMU, 20 kV, SE+BSE detectors) equipped with an energy dispersion spectrometer (EDS, Oxford Instruments, 20mm2)

   Principle of SEM: A scanning electron microscope scans a beam of electrons over a specimen to produce a magnified image of an object. Accelerated electrons in an SEM carry significant amounts of kinetic energy, and this energy is dissipated as a variety of signals produced by electron-sample interactions that can be used to obtain information about the surface topography and composition. A detector registers these scattered electrons and turns them into a picture.

2.3 Design of Experiments

In order to study the crystallization process of $CaSO_4$ batch experiments were conducted with solutions at different molar concentrations of $CaSO_4$, and the maximum and minimum concentration solutions were considered for the study under the influence of the addition of metal ions. The molar concentrations considered were in the range from 0.04 M/L to 0.08 M/L which correspond also to the supersaturation in the range 2.2 to 4.5. The supersaturation levels were derived from the calcium sulphate dihydrate solubility in water, which is 0.24 g/100 ml at 20ºC. This is equivalent to 0.018 M of gypsum dissolved in a litre of pure/distilled water.

2.4 Preparation of solutions

Calcium Sulphate solutions at different concentrations within the mentioned range were prepared from the stock solutions of Calcium Chloride and Sodium Sulphate. The stock solutions of volume 0.5-1 L were prepared from the salts, Calcium Chloride ($CaCl_2$) and Sodium Sulphate (Na_2SO_4), and deionised/distilled water at twice the required gypsum concentrations using the mass concentration (g/L) relative to the desired molar concentration. The mass concentration required is calculated using the following equation:

$$Mass\ concentration(\rho i)\ in\ g/l = \frac{Required\ Molarity\ X\ Molar\ Mass(M)\ X\ Required\ volume}{1000} \quad (7)$$

Table 2: Mass concentrations of CaCl2 and Na2SO4 solutions corresponding to the respective molar concentrations.

	Molar concentration (M/L)	**Mass concentration (g/L)**
$CaCl_2$	0.08	8.88
	0.1	11.10
	0.12	13.32
	0.14	15.54
	0.16	17.76
Na_2SO_4	0.08	11.36
	0.1	14.20
	0.12	17.04
	0.14	19.89
	0.16	22.73

These solutions of Calcium Chloride and Sodium Sulphate of same molar concentration are mixed together in equal volumes to get Calcium Sulphate solution of desired concentration.

2.5 Experimental set-up (beaker/jar tests)

Portions of the calibrated solutions of Calcium Sulphate equivalent to 100 ml at different concentrations are transferred to glass beakers of volume 250 ml each, periodically one after other. A magnet is suspended into the beaker and a conductivity meter is immersed in the beaker to measure the conductivity over a period of time. Then the beaker is placed on the magnetic stirrer turning at a speed of 200 rpm which ensures homogeneous mixing of the solution. The conductivity meter is further connected to the computer through a module and the values of conductivity are recorded onto a SQL database by using the EBS 20M software which are later exported as excel files.

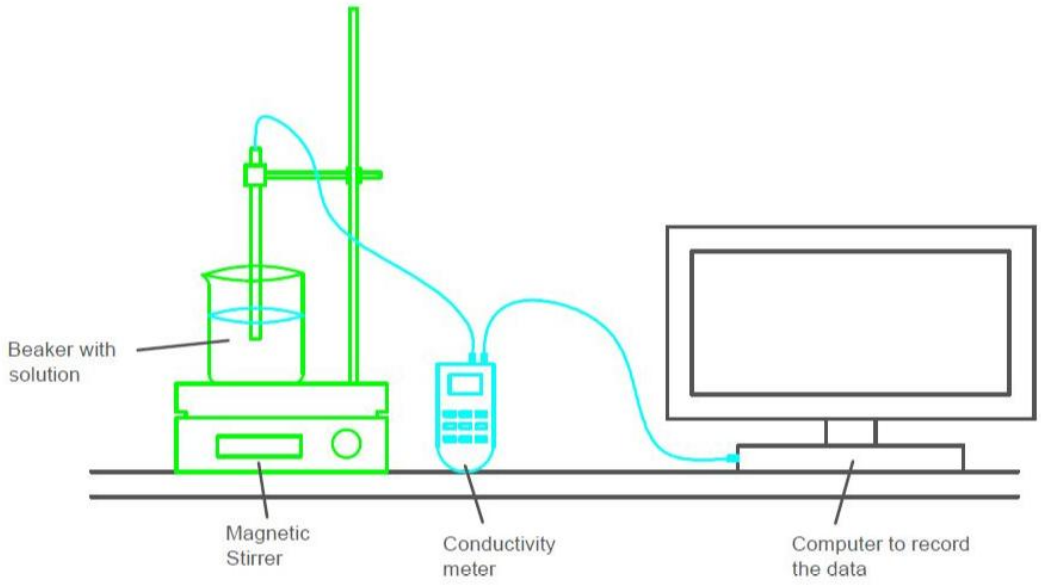

Figure 17: Experimental set-up of the beaker/jar test

Firstly, series of observations are carried out as per the above-mentioned procedure, using the solutions at different concentrations without the addition of metal ions/compounds. Each experimental record is carried out for a period of 3 hours. Later, metal compounds at different concentrations are added to the solutions of maximum (0.08 M/L) and minimum (0.05 M/L) concentrations, and the process is repeated. To introduce Zinc (Zn^{2+}), Zinc Chloride ($ZnCl_2$) is used and for Manganese (Mn^{2+}), Manganese Chloride monohydrate ($MnCl_2.H_2O$) is used. The addition of metal ions is done in accordance with the molar ratio. The molar ratios considered were 50:1; 100:1 and 200:1 with respect to the concentration of Calcium Sulphate solutions. The experiment is repeated with these solutions with additives and respective changes in conductivity are also recorded which are later compared.

Table 3: Mass concentration in mg/L of metal ions compounds added corresponding to the respective molar concentration ratio

CaSO4 concentration (M/L)	ZnCl2 in mg/L (for Zn in the ratio 200:1)	ZnCl2 in mg/L (for Zn in the ratio 100:1)	ZnCl2 in mg/L (for Zn in the ratio 50:1)
0.05	34.18	68.35	136.29
0.08	54.52	109.03	218.06
	MnCl2.H2O in mg/L (for Mn in the ratio 200:1)	MnCl2.H2O in mg/L (for Mn in the ratio 100:1)	MnCl2.H2O in mg/L (for Mn in the ratio 50:1)
0.05	35.97	71.93	143.86
0.08	57.54	115.08	230.18

2.6 Collection of Samples for SEM

After the end of each cycle, small drop-samples are collected and dried on the circular adhesive carbon tabs, which are later observed and analysed for the morphology and composition of the crystals formed under the SEM.

Chapter 3: Results and Discussion

3.1 Crystallization process

Precipitation studies without metal ions:

Five different calcium sulphate solutions of varying concentrations in the range 40 mmol/L – 80 mmol/L, corresponding to supersaturation range of 2.2 – 4.5 were investigated for precipitation behaviour under near constant physical conditions. The recorded values of conductivity over a 3-hour period are plotted onto a graph to study the relative crystallization process. Supersaturation of any degree in a solution would eventually lead to the precipitation of the excess dissolved ions into salts and promote crystal growth. This is turn would reduce the conductivity of the solution over a period of time. The part of time where the conductivity remains constant at a certain level before decreasing substantially from that point can be termed *induction period,* and that is when the crystal nucleation starts, ultimately leading to scaling [76].

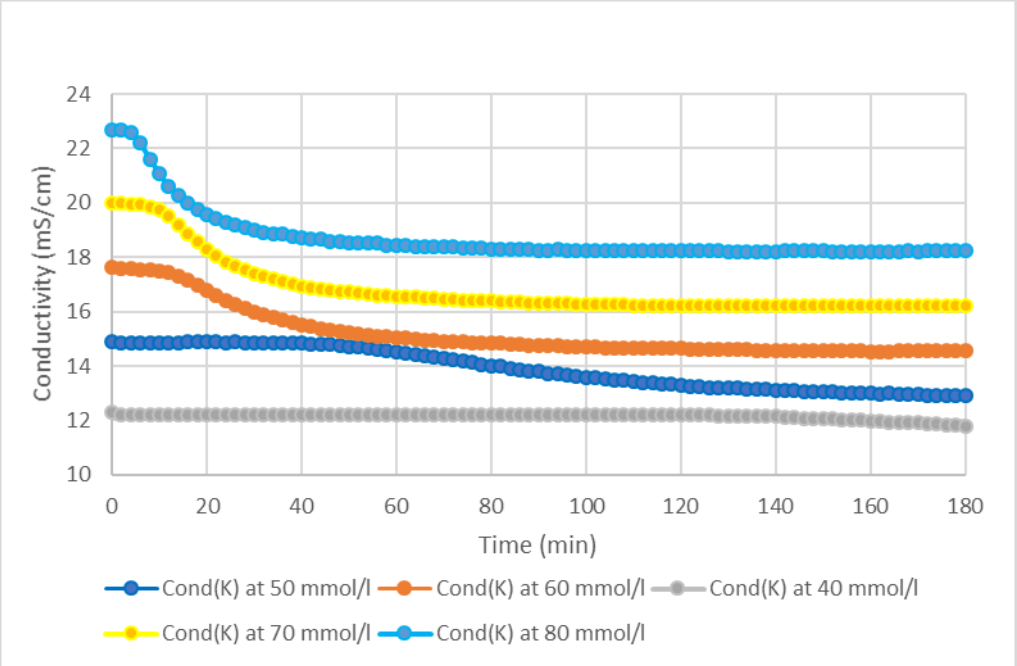

Figure 18: Rate of change of conductivity indicative of rate of precipitation at different supersaturations of Calcium Sulphate solutions (without metal ions)

From the graph (Fig.18) it can be observed that near-spontaneous precipitation or homogeneous nucleation prevails as the concentration of the solution goes higher. In the solutions of lower concentrations there is a considerable amount of time being lapsed before

we can see any changes in the conductivity. In such cases, most of the time it is an exogenous surface that stimulates heterogeneous nucleation, which could be a membrane surface.

Precipitation studies with the addition of metal ions - Zinc:

Calcium sulphate solution concentrations studied under the influence of metal ions were 50 mmol/L and 80 mmol/L. As before, the solutions were prepared from equal volumes of respective concentrations of $CaCl_2$ and Na_2SO_4. Firstly, the influence of Zn^{2+} is studied at varying molar concentration ratios of 50:1, 100:1 and 200:1 with respect to the $CaSO_4$ solution concentration. The zinc ions were introduced by mixing a relevant amount of Zinc Chloride - amount corresponding to the calculated ratio, as indicated in Table.3. Then the experimental procedure is carried out as before for all the six samples (three ratios each at two different calcium sulphate solution concentrations), and changes in the conductivity are recorded.

Zn^{2+} in 50 mmol/L $CaSO_4$ solution:

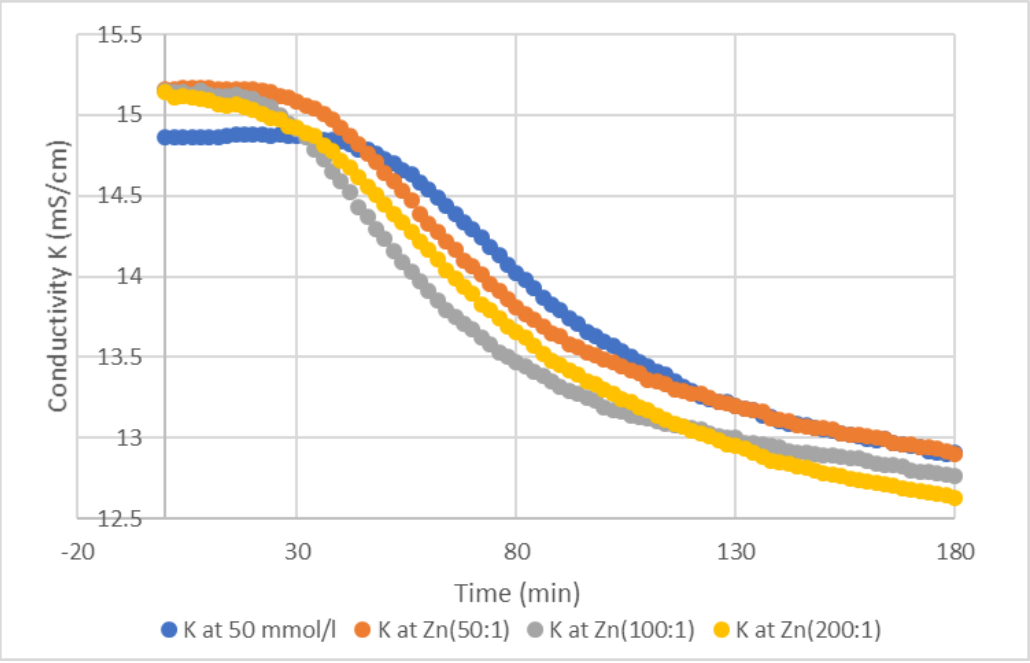

Figure 19: Rate of change of conductivity indicative of rate of precipitation at different molar ratios of Zn2+ in 50 mmol/L CaSO4 solution

The nucleation in beaker/jar tests occur in the bulk solution rather than on the surface. From the graph (Fig.19) obtained we can observe that due to the addition of zinc in the form of zinc chloride there is an increase in the initial conductivity of the solution. The change remains almost constant through the different molar ratios. The time lapsed until we see a

substantial decrease in the conductivity, induction time, is reduced to almost half through each iteration of concentration ratio from 50:1 till 200:1 (Table.4). This is in contrast to the findings from previous studies that as the concentration of additive ions increases, the active growth sites on the crystal surfaces may be blocked through adsorption and the rate of precipitation decreases [73] [74]. It is interesting to note that the nucleation is accelerated at lower concentrations of Zn^{2+} ions. This is a peculiar observation which needs to be further studied through repetition of experiments.

Table 4: Induction time corresponding to the molar ratio concentration of Zn2+

$CaSO_4$: Zn^{2+} (molar ratio)	Induction time (min)
Without Zn	40
50:1	20
100:1	18
200:1	6

It can also be observed that the time taken to reach stable state of supersaturation, where there is no further decrease in the conductivity, value is much longer.

Zn^{2+} in 80 mmol/L $CaSO_4$ solution:

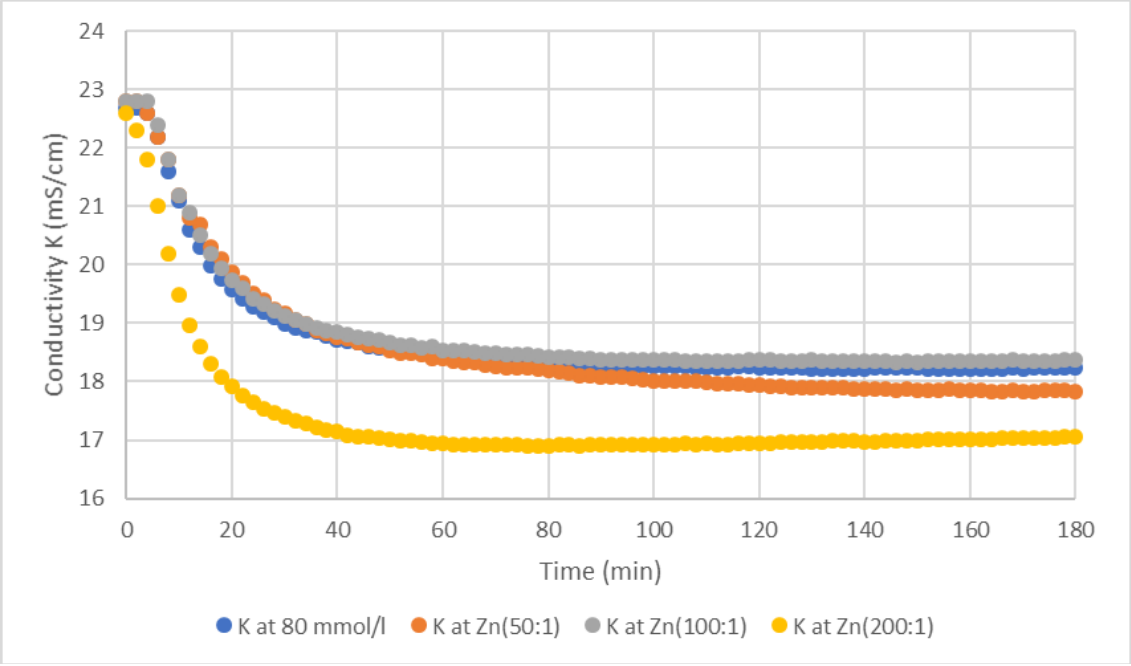

Figure 20: Rate of change of conductivity indicative of rate of precipitation at different molar ratios of Zn2+ in 80 mmol/L CaSO4 solution

As discussed previously, at higher solution concentrations above the threshold supersaturation there is an immediate nucleation facilitated by the abundance of ions which is homogeneous in nature. This is further hastened by the addition of zinc. From the graph we can also infer that the initial conductivity remains constant even after the addition of zinc chloride. It can also be observed that at higher solution concentration, the time taken to reach a stable state of supersaturation is very short in comparison to the solutions at lower solution concentrations.

Precipitation studies with the addition of metal ions - Manganese:

As stated earlier, the influence of Manganese (Mn^{2+}) ions on calcium sulphate solutions of concentrations 50 mmol/L and 80 mmol/L is studied in relation to the measured conductivity of the respective solutions over time (3 hours). Similar to zinc ions, the intended molar concentration of manganese ions is derived from the concentration ratios in relevance with the $CaSO_4$ solution concentrations. The manganese ions were introduced by mixing amounts of manganese chloride monohydrate ($MnCl_2.H_2O$) - amount corresponding to the calculated ratio, as indicated in Table.3. Then the experimental procedure is carried out as before for all the six samples (three ratios each at two different calcium sulphate solution concentrations), and changes in the conductivity are recorded, similar to the case of zinc addition.

Mn^{2+} in 50 mmol/L $CaSO_4$ solution:

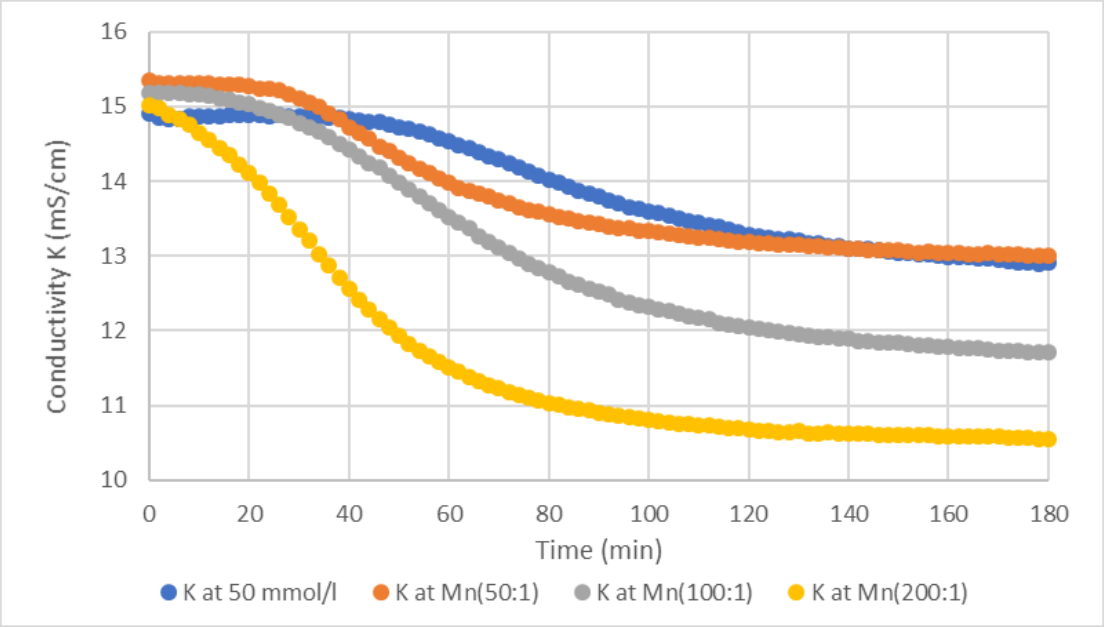

Figure 21: Rate of change of conductivity indicative of rate of precipitation at different molar ratios of Mn2+ in 50 mmol/L CaSO4 solution

As in case of zinc, an increase in the initial conductivity of the solution is observed on the addition of Mn^{2+}. There is a slight difference within the solutions of different concentration ratios with 50:1 having the maximum increase, which decreases as it comes to 200:1. The trend of induction time remains similar to that of zinc at the same $CaSO_4$ solution concentration, but a steep decrease can be noted with 50:1, 100:1 Mn^{2+} concentrations, while a very little amount of Mn^{2+} facilitates homogeneous nucleation resulting in immediate precipitation without any induction period (Table.5).

Table 5: Induction time corresponding to the molar ratio concentration of Mn2+

$CaSO_4$: Mn^{2+} (molar ratio)	Induction time (min)
Without Zn	40
50:1	16
100:!	6
200:1	0

The time to reach stable state of supersaturation is much less in the solution with the least Mn^{2+} ions. Also, there is a substantial difference in the decrease of conductivity between the three ratios, which may also indicate greater or increased level of precipitation/crystallization. The reasons for this are to be investigated further.

Mn^{2+} in 80 mmol/L $CaSO_4$ solution:

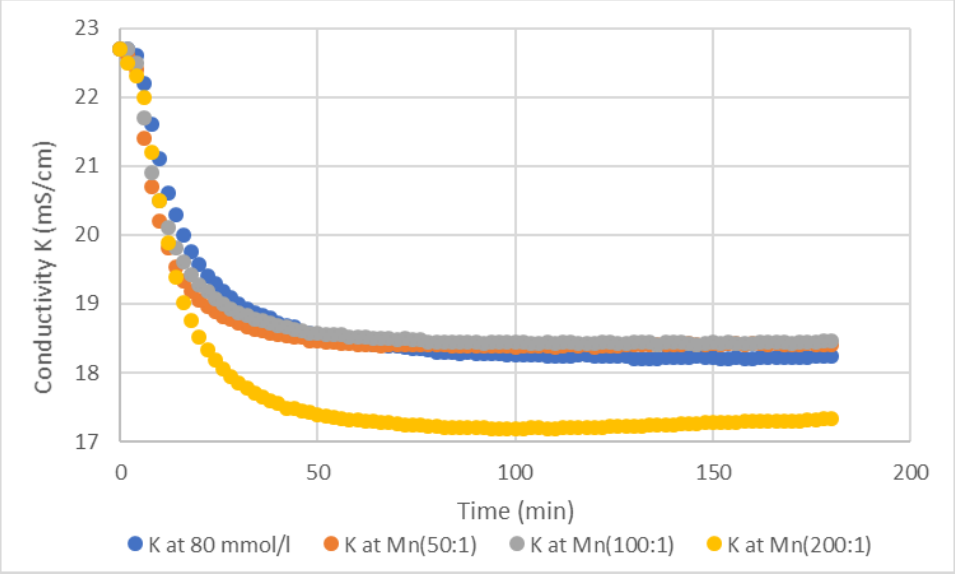

Figure 22: Rate of change of conductivity indicative of rate of precipitation at different molar ratios of Mn2+ in 80 mmol/L CaSO4 solution

The observations in this case, of Mn^{2+} in $CaSO_4$ solution concentration of 80 mmol/L are identical to the observations made in case of Zn^{2+}. The major difference being the initial conductivity level. There is no change in the initial conductivity of the solution on the addition of Mn^{2+} through manganese chloride monohydrate ($MnCl_2.H_2O$). Due to the supersaturation that exceeds the threshold supersaturation, there is an instantaneous nucleation and the conductivity starts decreasing right from the start, indicating the formation of crystals. Similar to all other samples, a peculiar behavior where the smallest ratio addition causes the maximum decrease of conductivity, and thereby being indicative of increased crystallization can also be observed here.

3.2 Crystal morphology and elemental distribution – SEM with EDS

For scanning electron microscopy (SEM), solution samples were collected onto carbon based, electrically conductive, double sided adhesive discs, dried and sputtered with gold (approximately 2 nm). They are studied under electron scanning microscopy (SEM, Tescan VEGA 3-LMU, 20 kV, SE+BSE detectors) equipped with an energy dispersion spectrometer (EDS, Oxford Instruments, 20mm2). Primary study was focussed on the concentrations which were analysed for crystallization under the influence of metal ions (both zinc and manganese), 50 mmol/L and 80 mmol/L. Pictures were captured at magnifications of 1000 (1.00k) and 5000 (5.00k) times. Also, due to the time constraint only the samples with $CaSO_4$ to metal ions ratios of 50:1 and 200:1 are observed for morphology and composition under the microscope.

Without the addition of metal ions:

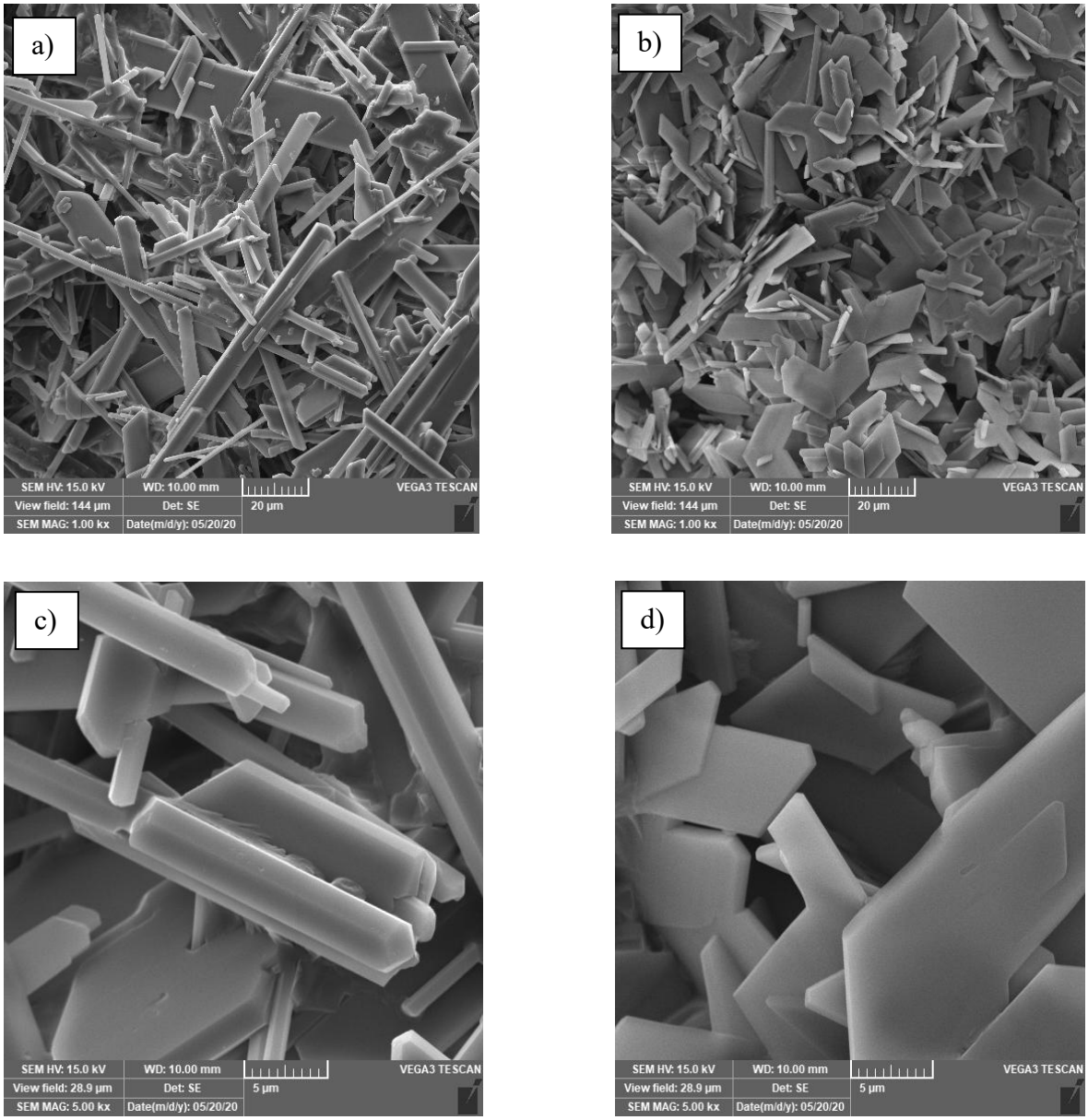

Figure 23: Morphology of CaSO4 crystals - a) 50 mmol/L at 1.00k magnification; b) 80 mmol/L at 1.00k magnification; c) 50 mmol/L at 5.00k magnification; d) 80 mmol/L at 5.00k magnification

From Fig.23, we can observe there is a noticeable difference in the crystal morphology of calcium sulphate crystals at different concentrations. This can be attributed to the immediate nucleation (homogeneous) that occurs at higher concentrations, above the threshold supersaturation. The crystals from the sample of 50 mmol/L $CaSO_4$ solution concentration are in shape of *rods*, while those formed at 80 mmol/L concentration are *rhombohedron* (flakes) in shape.

With the addition of Zinc (Zn^{2+}):

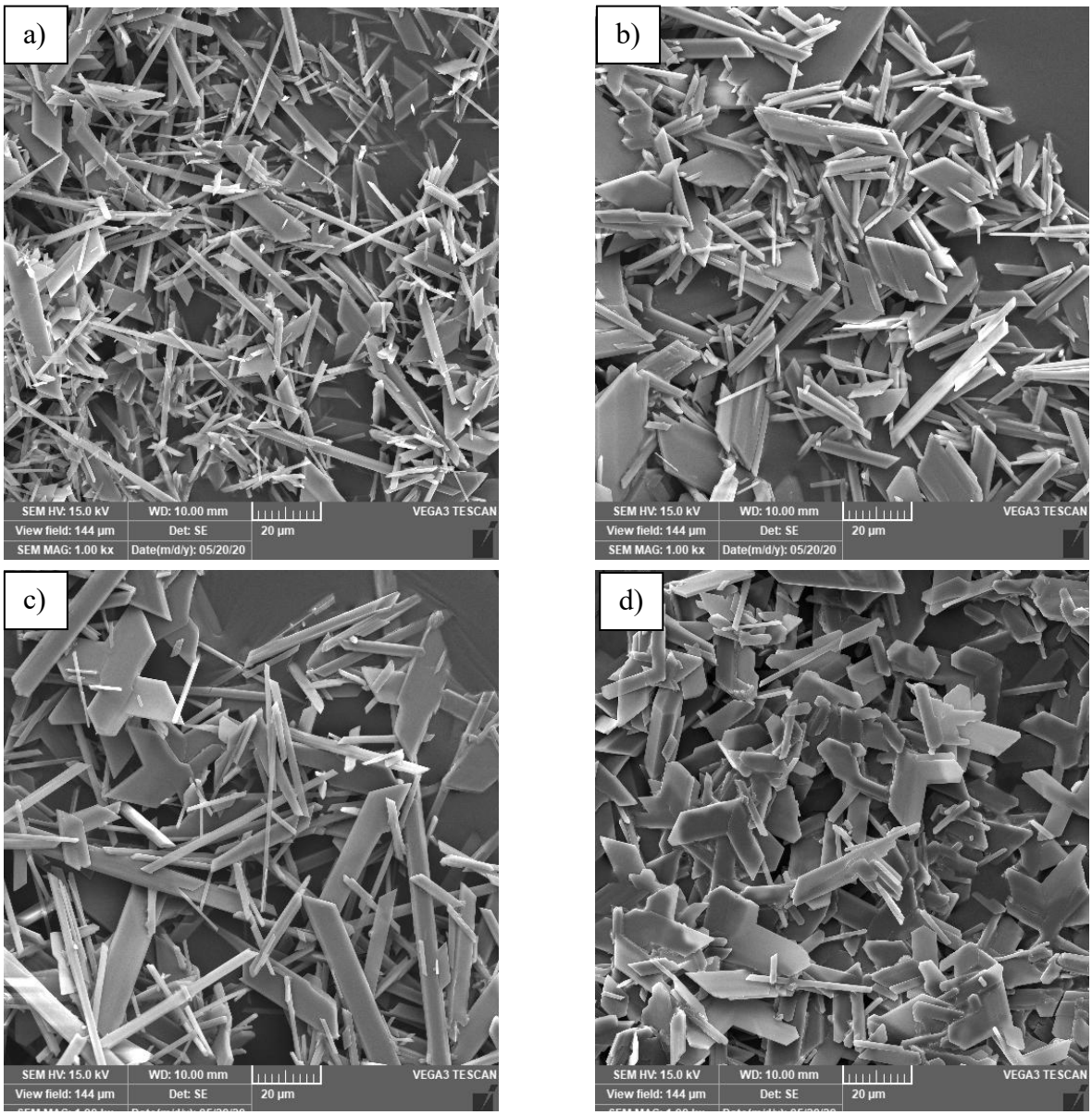

Figure 24: Morphology of CaSO4 crystals - a) 50 mmol/L and 50:1 Zn2+ at 1.00k magnification; b) 80 mmol/L and 50:1 Zn2+ at 1.00k magnification; c) 50 mmol/L and 200:1 Zn2+ at 1.00k magnification; d) 80 mmol/L and 200:1 Zn2+ at 1.00k magnification

On the addition of Zn^{2+}, there is a considerable change in the morphology that can be observed. Occurance of very small *needle* like structures is observed at both concentrations. But, the density of the needle shaped crystals is substantially more at higher concentration ratio 50:1 than at the lower ratio of 200:1. These samples are further analysed using EDS, to understand the elemental composition of the formed crystals and the possible influence of Zn^{2+} ions on the whole process.

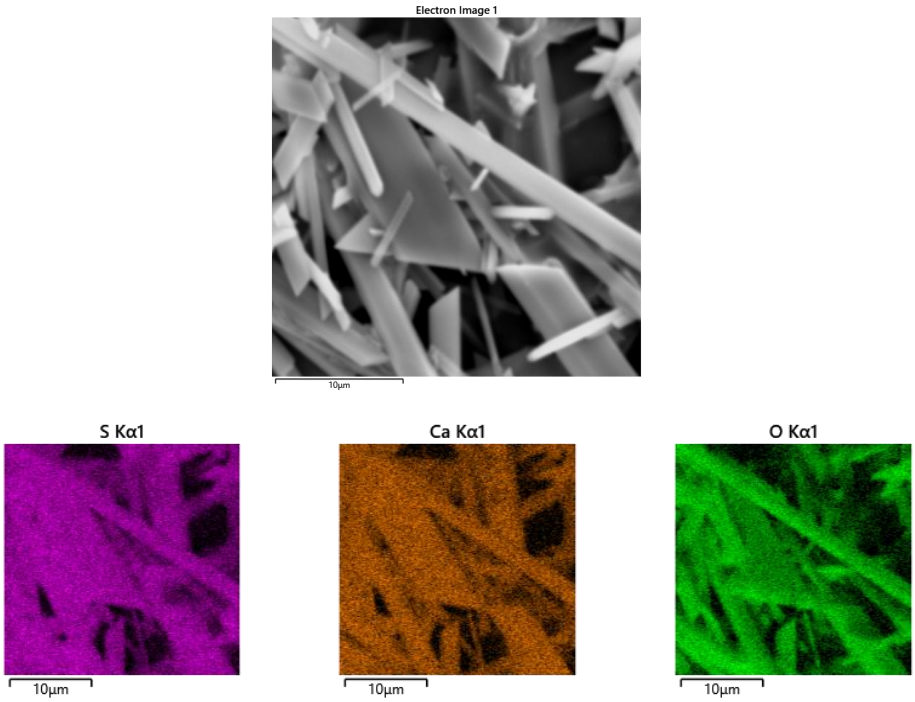

Figure 25: Elemental distribution of crystal sample of 50 mmol/L CaSO4 solution at 50:1 Zn2+

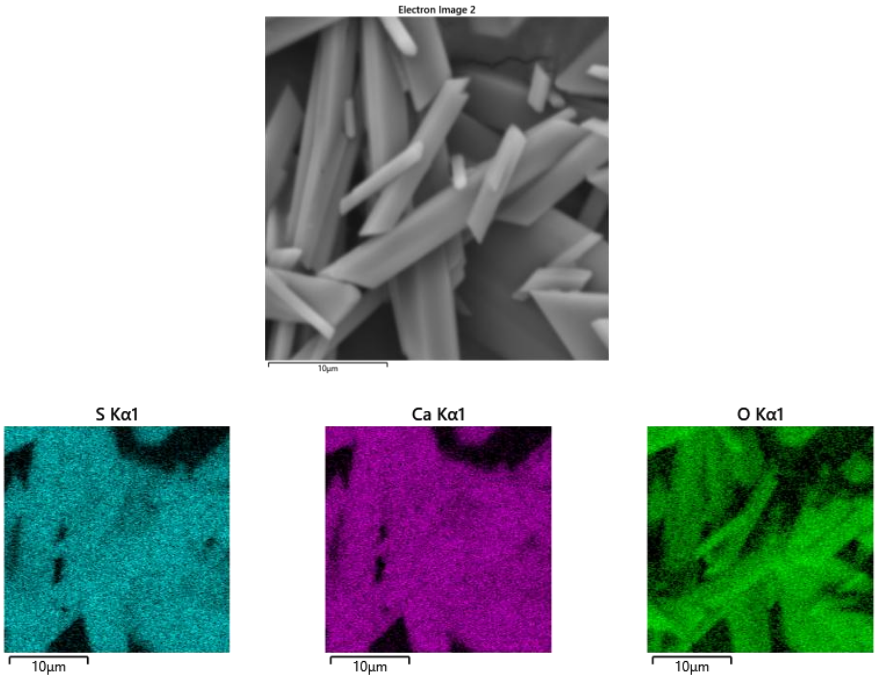

Figure 26: Elemental distribution of crystal sample of 80 mmol/L CaSO4 solution at 50:1 Zn2+

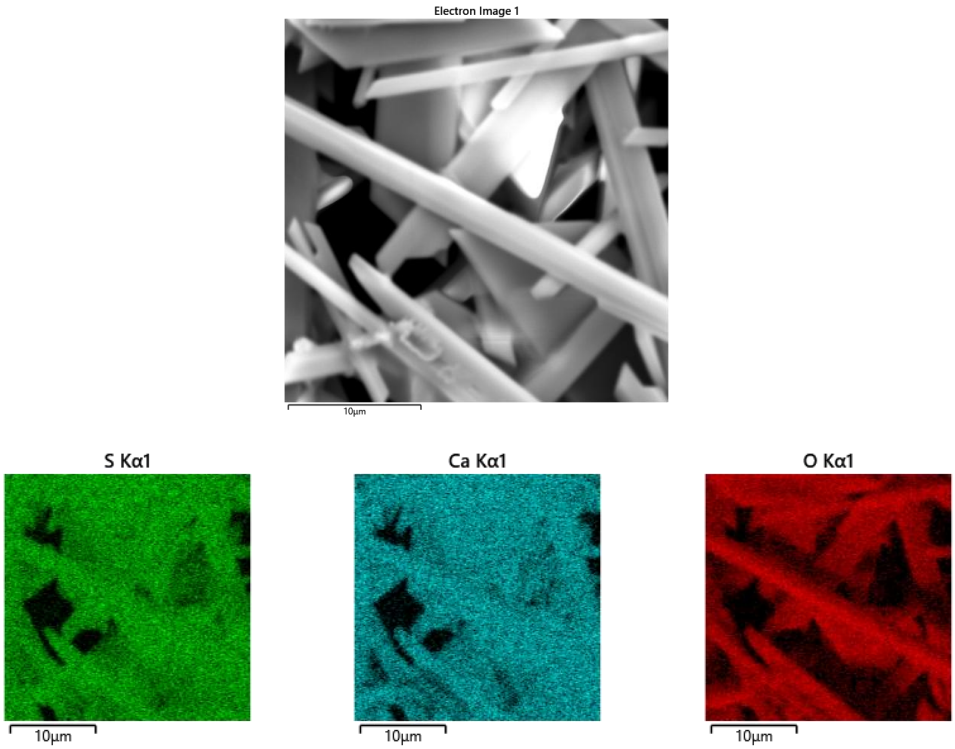

Figure 27: Elemental distribution of crystal sample of 50 mmol/L CaSO4 solution at 200:1 Zn2+

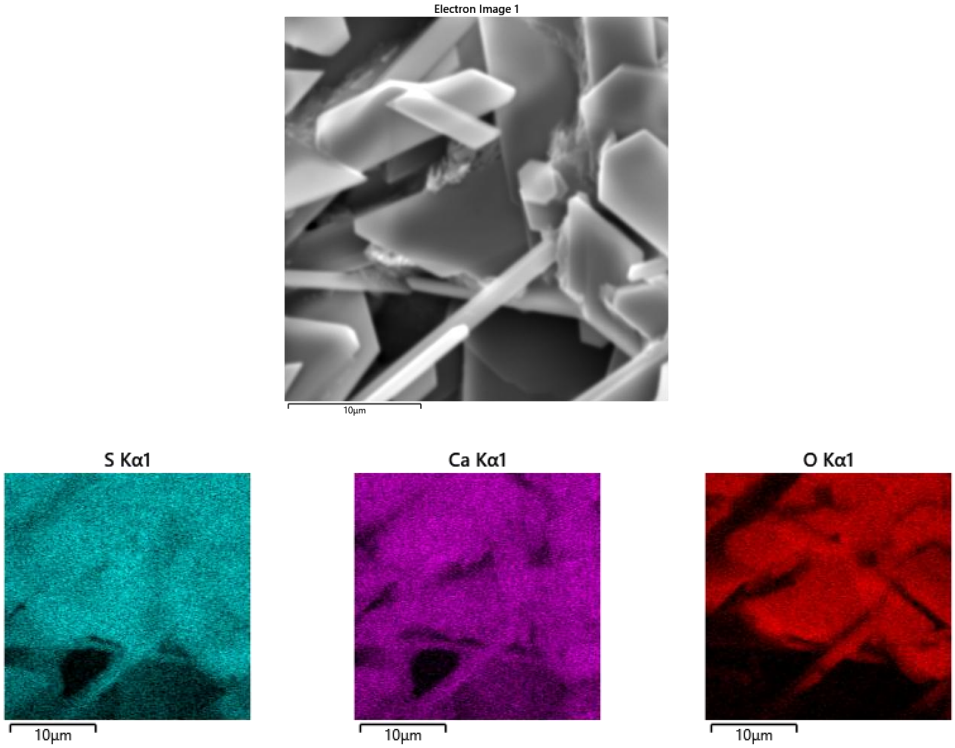

Figure 28: Elemental distribution of crystal sample of 80 mmol/L CaSO4 solution at 200:1 Zn2+

From the elemental distribution imagery, we can observe the crystal composition of $CaSO_4$ crystal samples on addition of Zn^{2+} at different concentration ratios. It shows the distribution of calcium (Ca), sulphur (S) and oxygen (O) within the crystal samples. During the analysis, small amounts of sodium (Na) and chloride (Cl) precipitates were also detected which is due to the initial salt reaction. The detection limit for bulk materials is 0.1 wt% therefore EDS cannot detect trace elements (concentrations below 0.01 wt%), which is the case for Zn^{2+} and hence was not detected. Nevertheless, from the crystal morphology study it is evident that the Zn^{2+} have a noticeable influence on the whole crystallization process.

With the addition of Manganese (Mn^{2+}):

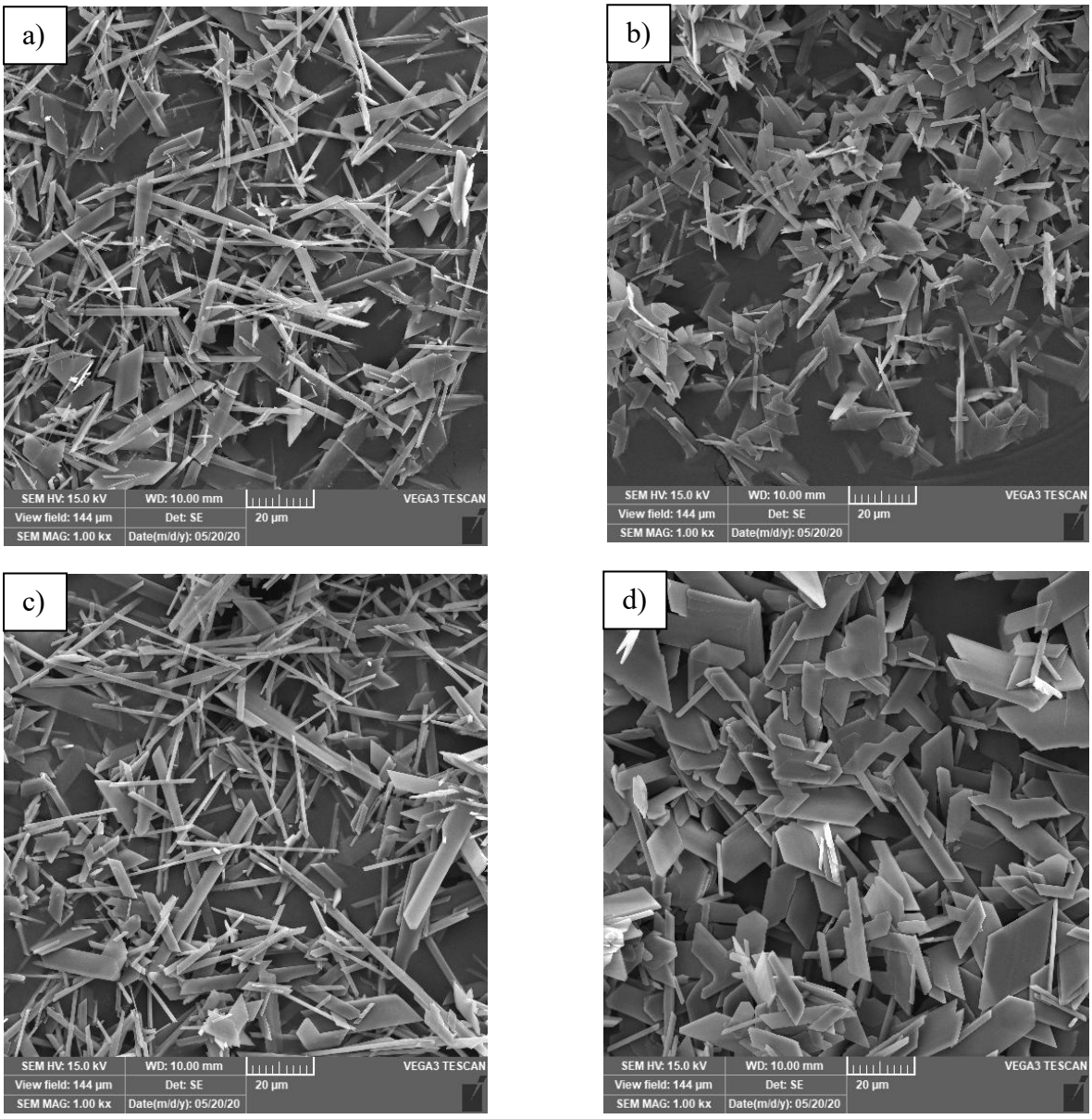

Figure 29: Morphology of CaSO4 crystals - a) 50 mmol/L and 50:1 Mn2+ at 1.00k magnification; b) 80 mmol/L and 50:1 Mn2+ at 1.00k magnification; c) 50 mmol/L and 200:1 Mn2+ at 1.00k magnification; d) 80 mmol/L and 200:1 Mn2+ at 1.00k magnification

The morphology observed under the influence of manganese (Mn^{2+}) is identical to the morphology observed in the samples with zinc. We can see the formation of thin *needle* shaped crystals which are of substantial amount in lower concentration $CaSO_4$ solution as compared to the higher concentration, similar to the case of zinc. These samples are also studied further to determine the elemental distribution.

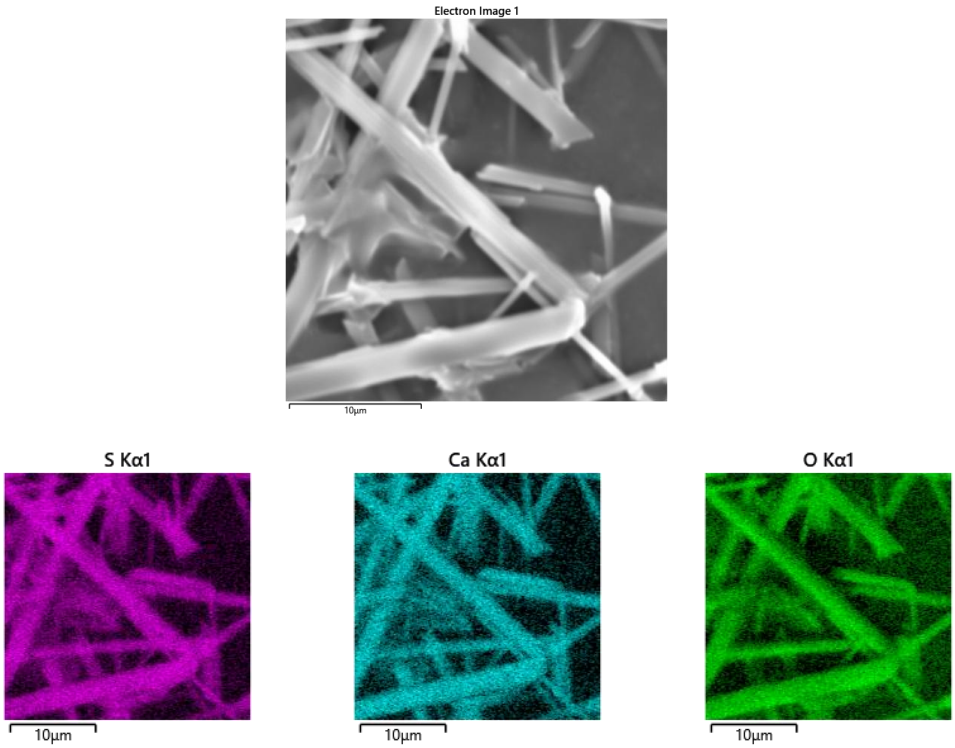

Figure 30: Elemental distribution of crystal sample of 50 mmol/L CaSO4 solution at 50:1 Mn2+

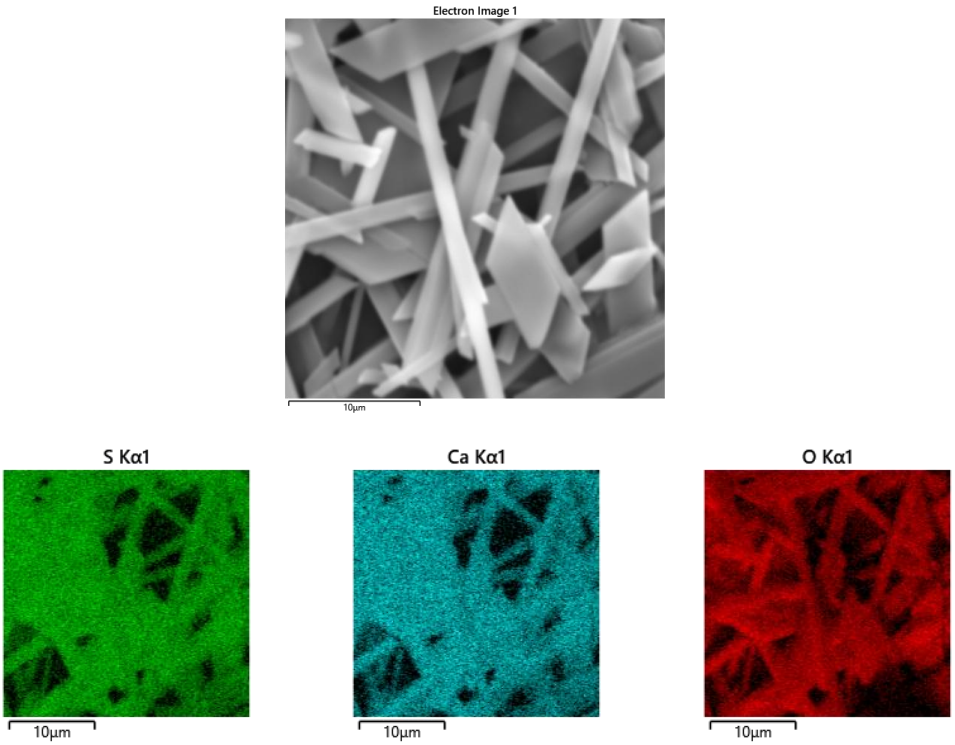

Figure 31: Elemental distribution of crystal sample of 50 mmol/L CaSO4 solution at 200:1 Mn2+

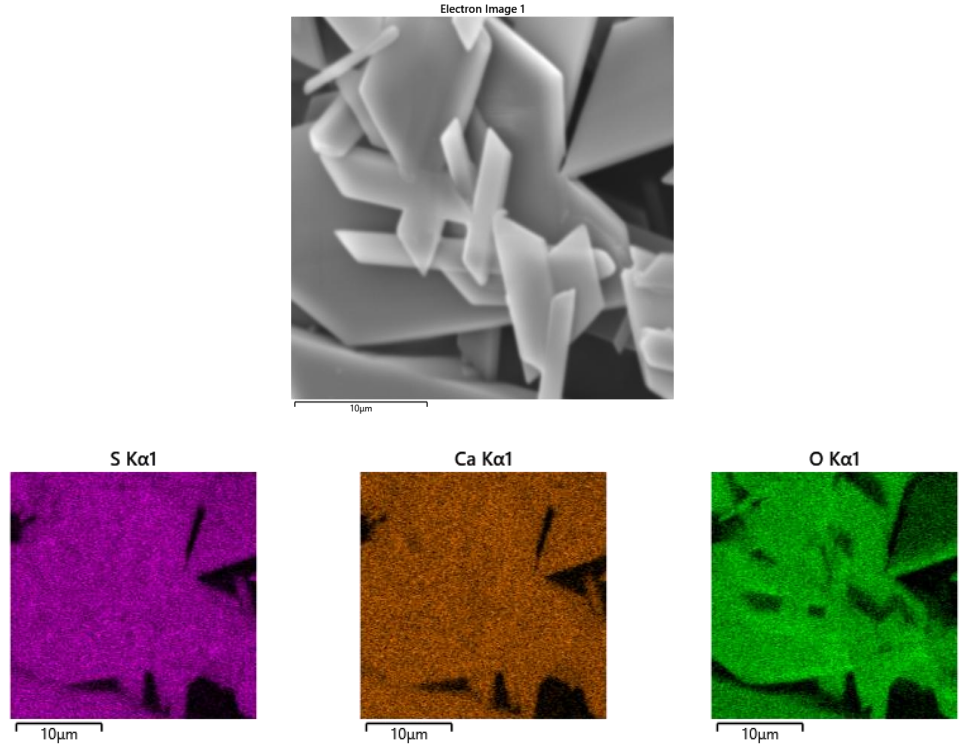

Figure 32: Elemental distribution of crystal sample of 80 mmol/L CaSO4 solution at 200:1 Mn2+

Different crystal samples with added manganese (Mn^{2+}) have been analysed for elemental distribution and the distribution maps for calcium (Ca), sulphur (S) and oxygen (O) were determined as in case of samples with added zinc ions. Similarly, the manganese content was not traceable as the detection limit of materials with EDS is 0.1 wt%, and that of manganese is much less than that. Though the presence of manganese could not be made evident through EDS, its influence can be affirmed based on the crystallization and morphological studies.

3.3 Limitations of the study

Though every effort has been made to carry out the intended research to its complete extent, it was not possible due to the lack of access to resources and time constraint. The crystallization process in all its phases from nucleation to the formation of mature crystals is strongly influenced by many factors, such as the presence of very small amount impurities, the temperature of the solution and even the nature of the surface of the beaker. Inaccuracies in weighing and further preparation of solutions may also be included. Also, the crystallization behaviour under varying physical conditions was not studied elaborately, but all these factors like temperature, pH, turbidity etc., were assumed to be constant throughout the whole process. It would be more convenient to work at a constant temperature and place the whole experimental set in a thermostat. Owing to the limited time again, the influence of metal ions on the crystallization process could be studied only at two concentration levels of all the intended solution concentrations. But the choice made provided with satisfactory results. It would be more appropriate to perform all experiments in triplicate, work with the average value and determine the standard deviations of the measurement. Most importantly, working with the membrane unit was not possible as it would require us setting it up, for which we did not have access to the required resources within the stipulated time.

Chapter 4: Conclusion and Recommendations

The importance of the study on the influence of the trace elements present in the feed water of desalination on the crystallization process of inorganic scalants, that in turn may effect the membrane scaling process has once again been established. More importantly, the differences in the nucleation processes and the altering rate of nucleation/crystallization of Calcium Sulphate dihydrate/Gypsum ($CaSO_4.2H_2O$) in the presence of specific metal ions (zinc and manganese) in homogenous solutions have been uncovered. The crystallization kinetics studied imply there is a reduction in the induction period on the addition of metal ions (Zn and Mn), thereby promoting faster precipitation. A peculiarity is observed in the molar concentration ratio addition of metals. At lower ratios (200:1), the nucleation was faster compared to higher concentration ratios (50:1) of gypsum to metal ions. The primary study did not include the study of crystallization under varying physical conditions such as (pH and temperature) and their influence on the process. This should be considered when continuing further studies.

The morphology of the crystal samples collected is studied under SEM. It is observed that there is a significant difference in crystal morphology at various solution concentrations of gypsum. The morphological study distinguished between *rod-like* and *flaky* crystal structures corresponding to lower and higher $CaSO_4$ solution concentrations respectively. The morphology is also altered by the addition of metal ions to a certain extent which is noticeable from the formation of needle like structures. Though there was a morphology change, the process of nucleation facilitating this change has not been analysed, which could be taken up going forward to better understand the reason for change, that eventually has an effect on the induction time.

During the elemental analysis by EDS, the trace amounts of zinc and manganese were not detected due to the measurable limit. But, it was observed there were a considerable amount of sodium and chloride elemental distribution as they are a by-product of reaction between the initial stock solutions of calcium chloride and sodium sulphate used to prepare calcium sulphate solutions. Going forward, it is advisable to filter these elements before analysing the sample for elemental distribution. Finally, it is recommended to carry out the experiments using the RO membrane unit which will give a clearer picture of the evaluation of the results obtained form the beaker/jar tests. This would facilitate in better understanding the influence of trace elements on membrane scaling and make necessary improvements.

Summary

The inherent aim of the experimental study carried out as part of the Master's degree thesis was to investigate the influence of trace metal ions on the crystallization process of Calcium Sulphate, especially in the form of Gypsum, which is a major inorganic scalant in membrane filtration process of Reverse Osmosis within desalination plants. Extensive preliminary review of various scientific articles was carried out to broaden the understanding of Inorganic scaling and to know the extent of studies carried out till date in the field of Reverse Osmosis membrane fouling. This gave a clearer perspective about the scale of research work being done on the impact of trace elements in the respective areas.

In our study, Calcium Sulphate solutions at two different concentrations under the influence of Zinc and Manganese metal ions were analysed by means of beaker/jar tests for conductivity curves, and crystallization rates were determined from the changes recorded over time. The metal ions were added in the amounts corresponding to the proposed molar ratios (50:1, 100:1, 200:1), relative to the $CaSO_4$ solution concentrations. The results recorded through EBS 20M are plotted on graphs which show a trend of decrease of induction time on the addition of Zn and Mn. A peculiarity is observed in all cases where smallest dosage (200:1) had the immediate and higher degree of influence in comparison to higher amount (50:1). Also, there is a notable difference in the morphology of the crystals formed. Formation of thin needle like structured crystals is observed to be substantial in the precipitate with the addition of the Zinc and Manganese. Though the elemental distribution of metals was not confirmed through EDS due to the detection limit, from morphological view point, we can infer that the concentration of trace metal ions of Zinc and manganese do interfere with the crystallization process of Calcium Sulphate that in turn may affect the rate of inorganic scaling on the membrane surface.

Though there were few substantial findings in the primary analysis, the intended study using a membrane unit was not carried out as it was not possible given the constraint of time and reduced accessibility under present circumstances. But, the data obtained will help to better set the process of reverse osmosis, where working with supersaturated solutions, knowledge of the rate of crystal formation is important, for example, to determine the maximum time of the solution in the device The data obtained is key to the further research that is planned. It will focus on the determination of direct scaling of the membrane with calcium sulphate in the presence of the tested metals.

References and Bibliography

1. **Seema S. Shenvi, Arun M. Isloor, A.F. Ismail.** 2015 February. A review on RO membrane technology: Developments and challenges; Desalination 368 (2015) 10–26.
2. **Shanxue Jiang, Yuening Li, Bradley P. Ladewig.** 8 April 2017. A review of reverse osmosis membrane fouling and control strategies; Science of the Total Environment 595 (2017) 567–583.
3. **Kaushik Nat**h. 2017. Membrane separation processes - 2nd edition, Delhi, PHI learning private limited.
4. **Richard W. Baker.** Membrane Technology and Applications - Wiley Publications. 2nd edition, Membrane Technology and Research, Inc. Menlo Park, California.
5. **Qian Liua,b, Guo-Rong Xuc, Rasel Das.** 26 July 2019. Inorganic scaling in reverse osmosis (RO) desalination: Mechanisms, monitoring, and inhibition strategies,
6. **Chien H. Tan, Olivier Lefebvre, Junyou Zhang, How Y. Ng and Say L. Ong.** June 2012, Membrane Processes for Desalination: Overview - DOI: 10.1061/9780784412275.ch10,
7. **Sagar Roy and Smruti Ragunath.** 1 November 2018. Emerging Membrane Technologies for Water and Energy Sustainability: Future Prospects, Constrains and Challenges - Department of Chemistry & Environmental Science, New Jersey Institute of Technology, Newark, NJ 07102
8. **Lorna Fitzsimons a, Brian Corcorana, Paul Young a, Greg Foley.** 8 January 2015, Exergy analysis of water purification and desalination: A study of exergy model approaches.
9. **Guo-Rong Xu, Jiao-NaWang, Cong-Ju Li**. 27 August 2013. Strategies for improving the performance of the polyamide thin film composite (PA TFC) reverse osmosis (RO) membranes: Surface modifications and nanoparticles incorporations, Desalination - 328 (2013) 83–100,
10. **P.S. Goh, W.J. Lau, M.H.D. Othman, A.F. Ismail.** 10 October 2017. Membrane fouling in desalination and its mitigation strategies – Desalination 2017.10.018
11. **Kurihara, M.; Takeuchi, H.** 2018. SWRO-PRO System in "Mega-ton Water System" for Energy Reduction and Low Environmental Impact. Water- 10, 48.
12. **Chesters, S.P**. 2009. Innovations in the inhibition and cleaning of reverse osmosis membrane scaling and fouling. Desalination 238:22–29.

13. **Al-Amoudi, A.S**., 2010. Factors affecting natural organic matter (NOM) and scaling fouling in NF membranes: a review. Desalination 259:1–10.
14. **Eric,M.V., Seungkwan, H.,Menachem, E.**, 2001. Influence of membrane surface properties on initial rate of colloidal fouling of reverse osmosis and nanofiltration membranes. Journal of Membrane Science. 188:115–128.
15. **Kochkodan, V., Johnson, D.J., Hilal, N.**, 2014. Polymeric membranes: surface modification for minimizing (bio)colloidal fouling. Advances in Colloid Interface Science. 206:116–140.
16. **Ahmad Fauzi Ismail, Kailash Chandra Khulbe, Takeshi Matsuura.** 2019. RO membrane fouling; Reverse Osmosis. – 189 to 220 Chapter-8. Elsevier Inc.
17. **A. Abdelrasoul, H. Doa, A. Lohi,** 2013. Fouling in Membrane Filtration and Remediation Methods, in: N. Nakajima (Ed.), Mass Transfer-Advances in Sustainable Energy and Environment Oriented Numerical Modeling, - pp. 195–216. Chapter 8 INTECH.
18. **S. Louie, I. Pinnau, I. Ciobanu, K.P. Ishida, A. Ng, M. Reinhard.** 2006. Effects of polyether polyamide block copolymer coating on performance and fouling of reverse osmosis membranes - J. Membrane Science. 280 762–770.
19. **Salahi, M. Abbasi, T. Mohammedi**. 2010. Permeate flux decline during UF of oily wastewater - Desalination 251 153–160.
20. **R. Verbeke, V. Gómez, I.F.J. Vankelecom.** 2017. Chlorine-resistance of reverse osmosis (RO) polyamide membranes - Prog. Polym. Sci. 72. 1–15.
21. **A.J.KarabelasA.KaranasiouD.C.Sioutopoulos.** August 2017. Experimental study on the effect of polysaccharides on incipient membrane scaling during desalination - Desalination 2017.04.009; 15
22. **Shirazi, S., Lin, C.J., Chen, D.,** 2010. Inorganic fouling of pressure-driven membrane processes - a critical review. Desalination 250:236–248.
23. **C. Piyadasa, H.F. Ridgway, T.R. Yeager, M.B. Stewart, C. Pelekani, S.R. Gray, et al.,** 2017. The application of electromagnetic fields to the control of the scaling and biofouling of reverse osmosis membranes - a review, Desalination 418 19–34.
24. **Creber, S.A., Pintelon, T.R.R., Graf Von Der Schulenburg, D.A.W., Vrouwenvelder, J.S., Van Loosdrecht, M.C.M., Johns, M.L.,** 2010. Magnetic resonance imaging and 3D simulation studies of biofilm accumulation and cleaning on reverse osmosis membranes - Food Bioprod. Process. 88:401–408.

25. **Yu, W., Yang, Y., Graham, N.,** 2016. Evaluation of ferrate as a coagulant aid/oxidant pre-treatment for mitigating submerged ultrafiltration membrane fouling in drinking water treatment - Chem. Eng. J. 298:234–242.
26. **Ding, S., Yang, Y., Li, C., Huang, H., Hou, L.A.,** 2016. The effects of organic fouling on the removal of radionuclides by reverse osmosis membranes - Water Res. 95:174–184.
27. **Naidu, G., Jeong, S., Kim, S.J., Kim, I.S., Vigneswaran, S.,** 2014. Organic fouling behavior in direct contact membrane distillation - Desalination 347:230–239.
28. **Shen, J., Schafer, A.I.,** 2015. Factors affecting fluoride and natural organic matter (NOM) removal from natural waters in Tanzania by Nano filtration/reverse osmosis - Sci.Total Environ. 527–528:520–529.
29. **Teixeira, M.R., Sousa, V.S.,** 2013. Fouling of nanofiltration membrane: effects of NOM molecular weight and microcystins - Desalination 315:149–155.
30. **Fabris, R., Chow, C.W.K., Drikas, M., Eikebrokk, B.,** 2008. Comparison of NOM character in selected Australian and Norwegian drinking waters - Water Res. 42:4188–4196.
31. **Al-Amoudi, A., Lovitt, R.W.,** 2007. Fouling strategies and the cleaning system of NF membranes and factors affecting cleaning efficiency - Membrane. Science. 303:4–28.
32. **Zhu, X., Elimelech, M.,** 1997. Colloidal fouling of reverse osmosis membranes: measurements and fouling mechanisms - Environmental Science Technology 31:3654–3662.
33. **Khayet, M.,** 2016. Fouling and scaling in desalination - Desalination 393:1.
34. **Tang, C.Y., Chong, T.H., Fane, A.G.,** 2011. Colloidal interactions and fouling of NF and RO membranes: a review - Adv. Colloid Interf. Sci. 164:126–143.
35. **Ju, Y., Hong, S.,** 2014. Nano-colloidal fouling mechanisms in seawater reverse osmosis process evaluated by cake resistance simulator-modified fouling index Nano filtration - Desalination 343:88–96.
36. **Kim, Y., Elimelech, M., Shon, H.K., Hong, S.,** 2014. Combined organic and colloidal fouling in forward osmosis: fouling reversibility and the role of applied pressure - J. Membrane. Science. 460:206–212.
37. **Motsa, M.M.,Mamba, B.B., Thwala, J.M., Verliefde, A.R.,** 2017. Osmotic backwash of fouled FO membranes: cleaning mechanisms and membrane surface properties after cleaning - Desalination 402:62–71.

38. **Ning, R.Y., Troyer, T.L., Tominello, R.S.,** 2005. Chemical control of colloidal fouling of reverse osmosis systems - Desalination 172:1–6.
39. **J.M. Gohil, A.K. Suresh,** Chlorine attack on reverse osmosis membranes: mechanisms and mitigation strategies - J. Membr. Sci. 541) 108–126,
40. **M.E. Julius Glater, Seung-kwan Hong.** 1994. The search for a chlorine-resistant reverse osmosis membrane - Desalination 95. 325–345,
41. **Asif Matina, Faizur Rahmanb, Hafiz Zahid Shafic, Syed M. Zubair,** 2019. Scaling of reverse osmosis membranes used in water desalination: Phenomena, impact, and control; future directions - Desalination 455.135–157;
42. **J. Fernández-Sempere, F. Ruiz-Beviá, P. García-Algado, R. Salcedo-Díaz,** 2010. Experimental study of concentration polarization in a crossflow reverse osmosis system using digital holographic interferometry - Desalination 257. 36–45.
43. **W. Li, X. Su, A. Palazzolo, S. Ahmed, E. Thomas,** 2017. Reverse osmosis membrane, seawater desalination with vibration assisted reduced inorganic fouling - Desalination 417. 102–114.
44. **R. Bian, K. Yamamoto, Y. Watanabe,** 2000. The effect of shear rate on controlling the concentration polarization and membrane fouling - Desalination 131. 225–236, S0011-9164(00)90021-3.
45. **Saqib, J., Aljundi, I.H.,** 2016. Membrane fouling and modification using surface treatment and layer-by-layer assembly of polyelectrolytes: state-of-the-art review - J.Water Process Eng. 11:68–87.
46. **Kwon, B., Lee, S., Cho, J., Ahn, H., Lee, D., Shin, H.S.,** 2005. Biodegradability, DBP formation, and membrane fouling potential of natural organic matter: characterization and controllability - Environ. Sci. Technol. 39:732–739.
47. **S. Zhao, L. Zou, D. Mulcahy**. 2012. Brackish water desalination by a hybrid forward osmosis–nanofiltration system using divalent draw solute - Desalination 284. 175–181.
48. **A. Pe'rez-Gonza'lez, A.M. Urtiaga, R. Iba'ñez, I. Ortiz,** 2012. State of the art and review on the treatment technologies of water reverse osmosis concentrates, - Water Res. 46. 267–283.
49. **Kh.L. Tu, A.R. Chivas, L.D. Nghiem**, 2011. Effects of membrane fouling and scaling on boron rejection by nanofiltration and reverse osmosis membranes - Desalination 279. 269–277.

50. **M.C. Amiri, M. Samiei,** 2007. Enhancing permeate flux in a RO plant by controlling membrane fouling, Desalination 207 () 361–369.
51. **F. Reverberi, A. Gorenflo,** 2007. Three year operational experience of a spiral-wound SWRO system with a high fouling potential feed water - Desalination 203. 100–106.
52. **H.-J. Oh, Y.-K. Choung, S. Lee, J.-S. Choi, T.-M. Hwang, J.H. Kim,** 2009. Scale formation in reverse osmosis desalination: model development, Desalination 238. 333–346.
53. **P. Xu, C. Bellona, J.E. Drewes,** 2010. Fouling of nanofiltration and reverse osmosis membranes during municipal wastewater reclamation: membrane autopsy results from pilot-scale investigations - J. Membr. Sci. 353.111–121.
54. **K.L. Tua, L.D. Nghiem, A.R. Chivas,** 2010. Boron removal by reverse osmosis membranes in seawater desalination applications, Sep. Purif. Technol. 75. 87–101.
55. **S.K. Hamdona, R.B. Nessim and S.M. Hamza*.** 1992. Spontaneous precipitation of calcium sulphate dihydrate in the presence of some metal ions.
56. **Schneider, R.P., Ferreira, L.M., Binder, P., Ramos, J.R.,** 2005. Analysis of foulant layer in all elements of an RO train - J. Membr. Sci. 261:152–162.
57. **S. Lee, C. Lee.** 2000. Effect of operating conditions on CaSO4 scale formation mechanism in nanofiltration for water softening - Water Res. 34. 3854–3866.
58. **M. Zhang, D. Hou, Q. She, C.Y. Tang,** 2014. Gypsum scaling in pressure retarded osmosis: experiments, mechanisms and implications - Water Res. 48. 387–395.
59. **V. Eroini, A. Neville, N. Kapur, M. Euvrard.** 2013. New insight into the relation between bulk precipitation and surface deposition of calcium carbonate mineral scale - Desalin. Water Treat. 51 (4–6) 882–891.
60. **S. Lee, C.H. Lee,** 2005. Scale formation in NF/RO: mechanism and control, Water Sci. Technol. 51. 267–275.
61. **T. Østvold, P. Randhol**. 2001. Kinetics of CaCO3 scale formation. The influence of temperature, supersaturation and ionic composition, International Symposium on Oilfield Scale 2001 - United Kingdom, Society of Petroleum Engineers Inc.: Aberdeen,
62. **J.W. Mullin,** , 2001. Crystallization, Butterworth-Heinemann
63. **E. Arkhangelsky, F. Wicaksana, C. Tang, A.A. Al-Rabiah, S.M. Al-Zahrani, R. Wang,** 2012. Combined organic-inorganic fouling of forward osmosis hollow fibre membranes - Water Res. 46. 6329–6338.

64. **T.A. Hoang, H.M. Ang, A.L. Rohl,** 2009. Effects of organic additives on calcium sulphate scaling in pipes - Aust. J. Chem. 62. 927–933.
65. **S. Shirazi, C. Lin, S. Doshi, S. Agarwal, P. Rao,** 2006. Comparison of fouling mechanism by CaSO4 and CaHPO4 on Nano filtration membranes - Sep. Sci. Technol. 41. 2861–2882.
66. **D. Freyer, W. Voigt,** 2003. Crystallization and phase stability of CaSO4 and CaSO4 –based salts - Monatshefte feur Chemie 134 . 693–719.
67. **T.A. Hoang, H.M. Ang, A.L. Rohl,** 2007. Effects of temperature on the scaling of calcium sulphate in pipes - Powder Technol. 179. 31–37.
68. **N.H. Lin, W.Y. Shih, E. Lyster, Y. Cohen,** 2011. Crystallization of calcium sulfate on polymeric surfaces - J. Colloid Interface Sci. 356. 790–797.
69. **S. Seewoo, R. Van Hille, A. Lewis,** 2004. Aspects of gypsum precipitation in scaling waters - Hydrometallurgy 75. 135–146.
70. **F. Rahman,** (2013) Calcium sulfate precipitation studies with scale inhibitors for reverse osmosis desalination - Desalination 319 79–84.
71. **J. Benecke, M. Haas, F. Baur, M. Ernst,** (2018) Investigating the development and reproducibility of heterogeneous gypsum scaling on reverse osmosis membranes using real-time membrane surface imaging - Desalination 428 161–171.
72. **J. Benecke, J. Rozova, M. Ernst,** (2018) Anti-scale effects of select organic macromolecules on gypsum bulk and surface crystallization during reverse osmosis desalination - Sep. Purif. Technol. 198 68–78.
73. **Samia K. Hamdona, Umaima A. Al Hadad;** 10 January 2007. Crystallization of calcium sulfate dihydrate in the presence of some metal ions; Journal of Crystal Growth 299 (2007) 146–151.
74. **Martin Bystrianský, Oded Nir, Marek Šír, ZuzanaHonzajková, Radek Vurma, Pavla Hrychová, Antonín Bervic, Bart van der Bruggen.** The presence of ferric iron promotes calcium sulphate scaling in reverse osmosis processes; Desalination 393 (2016) 115–119.
75. **Joseph A. Cotruvo**. August 2004. Desalination Guidelines Development for Drinking Water: Background - World Health Organization.
76. **Faizur Rahman**; 30 April 2013; Calcium sulfate precipitation studies with scale inhibitors for reverse osmosis desalination; Desalination 319 (2013) 79–84.
77. **Flemming, H.-C.**, 1997. Reverse osmosis membrane biofouling. Exp. Thermal Fluid Sci. 14:382–391.

Appendices

Appendix 1 – Measure of conductivity (K) at different $CaSO_4$ solution concentrations

Time (min)	Cond(K) at 50 mmol/l	Cond(K) at 60 mmol/l	Cond(K) at 40 mmol/l	Cond(K) at 70 mmol/l	Cond(K) at 80 mmol/l
0	14.91	17.63	12.31	20	22.7
2	14.85	17.58	12.23	19.97	22.7
4	14.83	17.57	12.22	19.96	22.6
6	14.83	17.56	12.21	19.93	22.2
8	14.86	17.56	12.22	19.87	21.6
10	14.86	17.5	12.22	19.74	21.1
12	14.86	17.43	12.21	19.51	20.6
14	14.87	17.31	12.21	19.21	20.3
16	14.88	17.15	12.23	18.88	19.99
18	14.88	16.96	12.21	18.56	19.76
20	14.89	16.78	12.21	18.29	19.58
22	14.88	16.6	12.21	18.04	19.41
24	14.87	16.42	12.22	17.83	19.29
26	14.88	16.28	12.22	17.67	19.19
28	14.87	16.13	12.22	17.52	19.09
30	14.87	16	12.22	17.4	18.99
32	14.87	15.89	12.22	17.3	18.93
34	14.86	15.79	12.22	17.19	18.87
36	14.85	15.69	12.22	17.1	18.84
38	14.85	15.6	12.22	17.02	18.79
40	14.84	15.52	12.21	16.95	18.72
42	14.82	15.45	12.21	16.9	18.69
44	14.79	15.39	12.21	16.85	18.66
46	14.79	15.33	12.21	16.79	18.6
48	14.76	15.28	12.21	16.75	18.58
50	14.73	15.24	12.21	16.72	18.55
52	14.7	15.18	12.21	16.67	18.53
54	14.66	15.14	12.22	16.65	18.52
56	14.63	15.11	12.22	16.62	18.51
58	14.58	15.08	12.22	16.58	18.46
60	14.54	15.05	12.21	16.56	18.46
62	14.49	15.02	12.21	16.55	18.46
64	14.44	14.98	12.22	16.53	18.41
66	14.39	14.96	12.22	16.5	18.41
68	14.34	14.94	12.22	16.49	18.38
70	14.29	14.91	12.22	16.45	18.38
72	14.24	14.91	12.22	16.44	18.37

Time (min)	Cond(K) at 50 mmol/l	Cond(K) at 60 mmol/l	Cond(K) at 40 mmol/l	Cond(K) at 70 mmol/l	Cond(K) at 80 mmol/l
74	14.18	14.89	12.22	16.43	18.35
76	14.13	14.87	12.22	16.42	18.35
78	14.07	14.86	12.22	16.39	18.34
80	14.02	14.84	12.22	16.39	18.3
82	13.98	14.83	12.22	16.37	18.3
84	13.93	14.8	12.22	16.36	18.3
86	13.87	14.79	12.22	16.34	18.28
88	13.83	14.78	12.22	16.33	18.29
90	13.79	14.76	12.22	16.31	18.27
92	13.74	14.75	12.22	16.31	18.27
94	13.71	14.74	12.22	16.3	18.28
96	13.66	14.73	12.22	16.3	18.27
98	13.63	14.71	12.22	16.28	18.25
100	13.6	14.7	12.22	16.27	18.26
102	13.57	14.69	12.22	16.27	18.25
104	13.54	14.68	12.22	16.27	18.26
106	13.5	14.68	12.22	16.25	18.26
108	13.47	14.67	12.22	16.25	18.24
110	13.44	14.67	12.21	16.24	18.24
112	13.41	14.66	12.21	16.23	18.24
114	13.39	14.66	12.21	16.22	18.24
116	13.35	14.65	12.2	16.22	18.25
118	13.32	14.65	12.2	16.22	18.25
120	13.29	14.64	12.19	16.22	18.24
122	13.26	14.62	12.21	16.22	18.24
124	13.24	14.61	12.2	16.22	18.24
126	13.22	14.61	12.2	16.23	18.24
128	13.22	14.6	12.18	16.23	18.24
130	13.2	14.6	12.17	16.22	18.21
132	13.18	14.6	12.16	16.22	18.21
134	13.17	14.6	12.15	16.23	18.21
136	13.14	14.59	12.14	16.22	18.21
138	13.13	14.59	12.15	16.22	18.22
140	13.1	14.59	12.14	16.22	18.22
142	13.09	14.58	12.13	16.21	18.23
144	13.09	14.58	12.11	16.21	18.23
146	13.08	14.58	12.09	16.21	18.24
148	13.06	14.58	12.07	16.22	18.23
150	13.05	14.57	12.07	16.22	18.23
152	13.04	14.57	12.06	16.22	18.21
154	13.03	14.57	12.04	16.22	18.21
156	13.02	14.57	12.02	16.22	18.22

Time (min)	Cond(K) at 50 mmol/l	Cond(K) at 60 mmol/l	Cond(K) at 40 mmol/l	Cond(K) at 70 mmol/l	Cond(K) at 80 mmol/l
158	13.01	14.56	12	16.22	18.21
160	12.99	14.54	11.98	16.24	18.21
162	12.98	14.54	11.96	16.24	18.22
164	12.99	14.54	11.95	16.23	18.22
166	12.97	14.55	11.93	16.23	18.22
168	12.96	14.55	11.93	16.23	18.23
170	12.95	14.55	11.91	16.23	18.22
172	12.94	14.55	11.89	16.22	18.23
174	12.92	14.55	11.87	16.22	18.23
176	12.91	14.55	11.84	16.24	18.24
178	12.9	14.55	11.82	16.24	18.24
180	12.91	14.56	11.8	16.24	18.24

Appendix 2 – Measure of conductivity (K) at 50 mmol/L $CaSO_4$ solution concentration with Zn^{2+} at various molar ratios

Time (min)	K at 50 mmol/l	K at Zn(50:1)	K at Zn(100:1)	K at Zn(200:1)
0	14.86	15.16	15.15	15.14
2	14.86	15.16	15.14	15.11
4	14.86	15.17	15.14	15.12
6	14.86	15.17	15.13	15.11
8	14.86	15.17	15.15	15.1
10	14.86	15.17	15.13	15.09
12	14.86	15.16	15.12	15.07
14	14.87	15.16	15.12	15.06
16	14.88	15.16	15.13	15.07
18	14.88	15.16	15.11	15.05
20	14.88	15.16	15.1	15.03
22	14.88	15.15	15.07	15.01
24	14.87	15.14	15.05	14.98
26	14.88	15.12	15	14.97
28	14.87	15.11	14.95	14.93
30	14.87	15.08	14.91	14.92
32	14.87	15.06	14.86	14.89
34	14.86	15.04	14.79	14.87
36	14.85	15.01	14.73	14.81
38	14.85	14.97	14.65	14.78
40	14.84	14.92	14.59	14.72
42	14.82	14.87	14.52	14.68
44	14.79	14.82	14.43	14.62
46	14.79	14.76	14.37	14.56
48	14.76	14.71	14.29	14.51
50	14.73	14.64	14.23	14.45
52	14.7	14.59	14.16	14.39
54	14.66	14.53	14.09	14.34
56	14.63	14.47	14.03	14.28
58	14.58	14.39	13.97	14.22
60	14.54	14.33	13.91	14.17
62	14.49	14.28	13.85	14.11
64	14.44	14.22	13.79	14.04
66	14.39	14.17	13.75	13.99
68	14.34	14.1	13.71	13.94
70	14.29	14.06	13.67	13.89
72	14.24	14.01	13.62	13.83
74	14.18	13.95	13.58	13.79
76	14.13	13.91	13.53	13.74
78	14.07	13.86	13.5	13.69
80	14.02	13.81	13.47	13.66

Time (min)	K at 50 mmol/l	K at Zn(50:1)	K at Zn(100:1)	K at Zn(200:1)
82	13.98	13.77	13.44	13.62
84	13.93	13.73	13.41	13.57
86	13.87	13.69	13.38	13.52
88	13.83	13.65	13.35	13.48
90	13.79	13.63	13.32	13.45
92	13.74	13.58	13.29	13.42
94	13.71	13.56	13.27	13.39
96	13.66	13.53	13.25	13.35
98	13.63	13.51	13.23	13.33
100	13.6	13.49	13.19	13.3
102	13.57	13.47	13.17	13.27
104	13.54	13.44	13.16	13.24
106	13.5	13.42	13.14	13.22
108	13.47	13.4	13.13	13.19
110	13.44	13.36	13.12	13.17
112	13.41	13.35	13.1	13.14
114	13.39	13.33	13.09	13.11
116	13.35	13.3	13.08	13.09
118	13.32	13.29	13.07	13.07
120	13.29	13.27	13.06	13.04
122	13.26	13.27	13.05	13.03
124	13.24	13.25	13.03	13.01
126	13.22	13.22	13.01	12.98
128	13.22	13.21	13	12.96
130	13.2	13.2	13	12.95
132	13.18	13.18	12.97	12.93
134	13.17	13.17	12.97	12.91
136	13.14	13.16	12.96	12.88
138	13.13	13.12	12.95	12.86
140	13.1	13.11	12.94	12.85
142	13.09	13.1	12.92	12.84
144	13.09	13.08	12.91	12.82
146	13.08	13.07	12.91	12.81
148	13.06	13.06	12.9	12.8
150	13.05	13.06	12.89	12.78
152	13.04	13.05	12.89	12.77
154	13.03	13.03	12.88	12.76
156	13.02	13.02	12.87	12.75
158	13.01	13.02	12.87	12.74
160	12.99	13.01	12.86	12.73
162	12.98	13	12.84	12.72
164	12.99	12.99	12.83	12.71
166	12.97	12.97	12.83	12.7

Time (min)	K at 50 mmol/l	K at Zn(50:1)	K at Zn(100:1)	K at Zn(200:1)
168	12.96	12.96	12.82	12.69
170	12.95	12.96	12.8	12.68
172	12.94	12.94	12.79	12.67
174	12.92	12.94	12.79	12.66
176	12.91	12.93	12.78	12.65
178	12.9	12.92	12.77	12.64
180	12.91	12.9	12.76	12.63

Appendix 3 – Measure of conductivity (K) at 80 mmol/L $CaSO_4$ solution concentration with Zn^{2+} at various molar ratios

Time (min)	K at 80 mmol/l	K at Zn(50:1)	K at Zn(100:1)	K at Zn(200:1)
0	22.7	22.8	22.8	22.6
2	22.7	22.8	22.8	22.3
4	22.6	22.6	22.8	21.8
6	22.2	22.2	22.4	21
8	21.6	21.8	21.8	20.2
10	21.1	21.2	21.2	19.49
12	20.6	20.8	20.9	18.97
14	20.3	20.7	20.5	18.6
16	19.99	20.3	20.2	18.31
18	19.76	20.1	19.94	18.09
20	19.58	19.87	19.73	17.91
22	19.41	19.7	19.59	17.77
24	19.29	19.52	19.43	17.65
26	19.19	19.4	19.32	17.53
28	19.09	19.23	19.22	17.46
30	18.99	19.16	19.12	17.39
32	18.93	19.06	19.05	17.32
34	18.87	18.98	18.99	17.28
36	18.84	18.88	18.91	17.22
38	18.79	18.83	18.87	17.16
40	18.72	18.75	18.84	17.14
42	18.69	18.73	18.8	17.09
44	18.66	18.68	18.76	17.06
46	18.6	18.63	18.73	17.05
48	18.58	18.59	18.72	17.03
50	18.55	18.54	18.67	17.01
52	18.53	18.48	18.63	16.99
54	18.52	18.48	18.62	16.98
56	18.51	18.46	18.58	16.96
58	18.46	18.4	18.59	16.95
60	18.46	18.39	18.54	16.94
62	18.46	18.36	18.54	16.93
64	18.41	18.34	18.53	16.93
66	18.41	18.32	18.5	16.91
68	18.38	18.28	18.49	16.92
70	18.38	18.27	18.48	16.91
72	18.37	18.24	18.46	16.91
74	18.35	18.23	18.46	16.91
76	18.35	18.23	18.46	16.9
78	18.34	18.21	18.44	16.89
80	18.3	18.19	18.43	16.89

Time (min)	K at 80 mmol/l	K at Zn(50:1)	K at Zn(100:1)	K at Zn(200:1)
82	18.3	18.18	18.43	16.91
84	18.3	18.14	18.41	16.91
86	18.28	18.11	18.4	16.9
88	18.29	18.11	18.4	16.91
90	18.27	18.09	18.38	16.91
92	18.27	18.08	18.38	16.91
94	18.28	18.07	18.38	16.92
96	18.27	18.05	18.38	16.92
98	18.25	18.04	18.37	16.92
100	18.26	18.02	18.37	16.93
102	18.25	18.01	18.37	16.92
104	18.26	18.02	18.37	16.93
106	18.26	18.01	18.35	16.94
108	18.24	18	18.35	16.93
110	18.24	17.99	18.35	16.94
112	18.24	17.97	18.36	16.93
114	18.24	17.97	18.36	16.93
116	18.25	17.96	18.36	16.94
118	18.25	17.94	18.37	16.94
120	18.24	17.94	18.37	16.94
122	18.24	17.91	18.37	16.95
124	18.24	17.92	18.35	16.96
126	18.24	17.9	18.36	16.96
128	18.24	17.9	18.36	16.96
130	18.21	17.89	18.37	16.96
132	18.21	17.9	18.35	16.97
134	18.21	17.9	18.35	16.98
136	18.21	17.9	18.35	16.98
138	18.22	17.88	18.36	16.98
140	18.22	17.88	18.36	16.96
142	18.23	17.87	18.35	16.97
144	18.23	17.87	18.36	16.98
146	18.24	17.86	18.34	16.98
148	18.23	17.87	18.35	16.98
150	18.23	17.85	18.34	17
152	18.21	17.86	18.35	17.01
154	18.21	17.86	18.36	17.01
156	18.22	17.87	18.36	17.01
158	18.21	17.85	18.36	17.01
160	18.21	17.86	18.36	17.01
162	18.22	17.86	18.36	17.01
164	18.22	17.83	18.36	17.01
166	18.22	17.84	18.36	17.03

Time (min)	K at 80 mmol/l	K at Zn(50:1)	K at Zn(100:1)	K at Zn(200:1)
168	18.23	17.85	18.37	17.03
170	18.22	17.84	18.36	17.03
172	18.23	17.84	18.35	17.04
174	18.23	17.85	18.36	17.04
176	18.24	17.85	18.36	17.04
178	18.24	17.85	18.37	17.05
180	18.24	17.84	18.37	17.05

Appendix 4 – Measure of conductivity (K) at 50 mmol/L $CaSO_4$ solution concentration with Mn^{2+} at various molar ratios

Time	K at 50 mmol/l	K at Mn(50:1)	K at Mn(100:1)	K at Mn(200:1)
0	14.91	15.35	15.18	15.02
2	14.85	15.32	15.19	14.98
4	14.83	15.31	15.19	14.89
6	14.83	15.32	15.19	14.83
8	14.86	15.32	15.17	14.75
10	14.86	15.32	15.16	14.65
12	14.86	15.31	15.14	14.56
14	14.87	15.3	15.11	14.44
16	14.88	15.3	15.09	14.35
18	14.88	15.29	15.05	14.23
20	14.89	15.27	15.03	14.11
22	14.88	15.24	14.98	13.99
24	14.87	15.23	14.95	13.84
26	14.88	15.21	14.89	13.68
28	14.87	15.16	14.85	13.52
30	14.87	15.11	14.78	13.36
32	14.87	15.05	14.73	13.21
34	14.86	14.99	14.66	13.03
36	14.85	14.9	14.59	12.87
38	14.85	14.83	14.5	12.71
40	14.84	14.73	14.43	12.57
42	14.82	14.65	14.33	12.42
44	14.79	14.58	14.25	12.28
46	14.79	14.47	14.18	12.15
48	14.76	14.4	14.08	12.04
50	14.73	14.32	13.99	11.93
52	14.7	14.25	13.89	11.83
54	14.66	14.17	13.8	11.74
56	14.63	14.11	13.71	11.65
58	14.58	14.03	13.62	11.58
60	14.54	13.98	13.53	11.51
62	14.49	13.91	13.44	11.45
64	14.44	13.87	13.37	11.39
66	14.39	13.83	13.26	11.32
68	14.34	13.79	13.19	11.27
70	14.29	13.74	13.11	11.23
72	14.24	13.71	13.04	11.18
74	14.18	13.65	12.97	11.14
76	14.13	13.62	12.89	11.11
78	14.07	13.59	12.84	11.07

Time	K at 50 mmol/l	K at Mn(50:1)	K at Mn(100:1)	K at Mn(200:1)
80	14.02	13.56	12.78	11.04
82	13.98	13.53	12.72	11.01
84	13.93	13.51	12.65	10.97
86	13.87	13.47	12.61	10.95
88	13.83	13.45	12.56	10.93
90	13.79	13.43	12.52	10.91
92	13.74	13.39	12.48	10.89
94	13.71	13.38	12.42	10.86
96	13.66	13.37	12.38	10.84
98	13.63	13.34	12.35	10.82
100	13.6	13.33	12.32	10.81
102	13.57	13.31	12.29	10.79
104	13.54	13.3	12.26	10.78
106	13.5	13.29	12.23	10.76
108	13.47	13.26	12.2	10.75
110	13.44	13.25	12.18	10.74
112	13.41	13.24	12.16	10.73
114	13.39	13.23	12.11	10.71
116	13.35	13.21	12.08	10.7
118	13.32	13.19	12.07	10.69
120	13.29	13.19	12.05	10.68
122	13.26	13.18	12.03	10.67
124	13.24	13.17	12.01	10.66
126	13.22	13.16	11.99	10.65
128	13.22	13.15	11.98	10.65
130	13.2	13.15	11.95	10.66
132	13.18	13.14	11.94	10.63
134	13.17	13.13	11.92	10.63
136	13.14	13.12	11.91	10.64
138	13.13	13.11	11.9	10.62
140	13.1	13.1	11.89	10.63
142	13.09	13.09	11.87	10.62
144	13.09	13.08	11.86	10.62
146	13.08	13.08	11.85	10.61
148	13.06	13.08	11.85	10.61
150	13.05	13.07	11.84	10.6
152	13.04	13.06	11.83	10.6
154	13.03	13.05	11.8	10.6
156	13.02	13.06	11.8	10.6
158	13.01	13.05	11.79	10.59
160	12.99	13.04	11.78	10.59
162	12.98	13.04	11.77	10.58
164	12.99	13.03	11.76	10.59

Time	K at 50 mmol/l	K at Mn(50:1)	K at Mn(100:1)	K at Mn(200:1)
166	12.97	13.02	11.76	10.58
168	12.96	13.04	11.75	10.58
170	12.95	13.03	11.74	10.58
172	12.94	13.02	11.74	10.57
174	12.92	13.02	11.73	10.57
176	12.91	13.01	11.72	10.57
178	12.9	13.01	11.72	10.56
180	12.91	13.01	11.72	10.56

Appendix 5 – Measure of conductivity (K) at 80 mmol/L $CaSO_4$ solution concentration with Mn^{2+} at various molar ratios

Time	K at 80 mmol/l	K at Mn(50:1)	K at Mn(100:1)	K at Mn(200:1)
0	22.7	22.7	22.7	22.7
2	22.7	22.6	22.7	22.5
4	22.6	22.4	22.5	22.3
6	22.2	21.4	21.7	22
8	21.6	20.7	20.9	21.2
10	21.1	20.2	20.5	20.5
12	20.6	19.81	20.1	19.88
14	20.3	19.53	19.82	19.39
16	19.99	19.33	19.61	19.01
18	19.76	19.18	19.42	18.75
20	19.58	19.06	19.28	18.51
22	19.41	18.96	19.18	18.33
24	19.29	18.89	19.08	18.19
26	19.19	18.81	19	18.05
28	19.09	18.77	18.92	17.94
30	18.99	18.73	18.87	17.86
32	18.93	18.66	18.83	17.78
34	18.87	18.63	18.78	17.71
36	18.84	18.61	18.76	17.65
38	18.79	18.57	18.72	17.6
40	18.72	18.56	18.69	17.56
42	18.69	18.53	18.67	17.49
44	18.66	18.52	18.63	17.48
46	18.6	18.51	18.61	17.44
48	18.58	18.47	18.58	17.42
50	18.55	18.47	18.57	17.39
52	18.53	18.45	18.56	17.37
54	18.52	18.44	18.55	17.36
56	18.51	18.42	18.55	17.34
58	18.46	18.42	18.52	17.32
60	18.46	18.41	18.52	17.31
62	18.46	18.41	18.52	17.3
64	18.41	18.41	18.5	17.29
66	18.41	18.39	18.5	17.28
68	18.38	18.4	18.49	17.27
70	18.38	18.4	18.48	17.26
72	18.37	18.41	18.49	17.25
74	18.35	18.41	18.48	17.24
76	18.35	18.41	18.48	17.24
78	18.34	18.4	18.44	17.22
80	18.3	18.4	18.45	17.22
82	18.3	18.41	18.45	17.21

Time	K at 80 mmol/l	K at Mn(50:1)	K at Mn(100:1)	K at Mn(200:1)
84	18.3	18.39	18.45	17.21
86	18.28	18.39	18.45	17.2
88	18.29	18.38	18.45	17.2
90	18.27	18.38	18.45	17.2
92	18.27	18.39	18.43	17.2
94	18.28	18.39	18.44	17.19
96	18.27	18.38	18.44	17.19
98	18.25	18.39	18.45	17.19
100	18.26	18.37	18.45	17.19
102	18.25	18.38	18.45	17.19
104	18.26	18.39	18.42	17.2
106	18.26	18.38	18.43	17.2
108	18.24	18.38	18.44	17.18
110	18.24	18.37	18.43	17.18
112	18.24	18.38	18.44	17.2
114	18.24	18.4	18.45	17.2
116	18.25	18.38	18.43	17.2
118	18.25	18.4	18.43	17.21
120	18.24	18.37	18.43	17.21
122	18.24	18.38	18.44	17.21
124	18.24	18.39	18.44	17.22
126	18.24	18.39	18.43	17.22
128	18.24	18.4	18.43	17.22
130	18.21	18.41	18.44	17.22
132	18.21	18.4	18.44	17.22
134	18.21	18.4	18.44	17.24
136	18.21	18.41	18.41	17.24
138	18.22	18.4	18.44	17.24
140	18.22	18.41	18.44	17.24
142	18.23	18.41	18.45	17.26
144	18.23	18.42	18.42	17.26
146	18.24	18.41	18.41	17.26
148	18.23	18.41	18.43	17.27
150	18.23	18.42	18.44	17.27
152	18.21	18.41	18.43	17.27
154	18.21	18.42	18.45	17.27
156	18.22	18.42	18.42	17.27
158	18.21	18.41	18.42	17.29
160	18.21	18.42	18.42	17.3
162	18.22	18.42	18.44	17.29
164	18.22	18.41	18.44	17.3
166	18.22	18.42	18.45	17.3
168	18.23	18.4	18.44	17.3
170	18.22	18.4	18.43	17.3

Time	K at 80 mmol/l	K at Mn(50:1)	K at Mn(100:1)	K at Mn(200:1)
172	18.23	18.41	18.45	17.3
174	18.23	18.42	18.45	17.31
176	18.24	18.4	18.45	17.31
178	18.24	18.41	18.46	17.33
180	18.24	18.41	18.46	17.33